Characterization of an efflux pump system, the CD_AcrA-AcrB-TolC complex, in *Clostridium difficile*

by

Jose M. Espinola Lopez

B.S., Kansas State University, 2015
B.A., Kansas State University, 2015

A THESIS

submitted in partial fulfillment of the requirements for the degree

MASTER OF SCIENCE

Interdepartmental Genetics Program
Department of Plant Pathology
College of Agriculture

KANSAS STATE UNIVERSITY
Manhattan, Kansas

2017

Approved by:

Major Professor
Dr. Revathi Govind

Copyright

Abstract

Clostridium difficile, a gram-positive, anaerobic bacterium, is a major cause of antibiotic-related diarrhea and pseudomembraneous colitis. In the last decades, *C. difficile* has emerged as a major threat because of its tendency to cause frequent and severe disease. Because of the severity of the infection and its high rate of recurrence, there is a significant financial burden on healthcare systems. Antibiotic treatments are a primary risk factor for the development of *C. difficile* infection because they disrupt the normal gut flora in the host, enabling the antibiotic resistant bacterium to colonize the colon. Most of the resistance mechanisms in *C. difficile* reported to date can be classified as either antibiotic-degrading enzymes or modification of target sites. Another mechanism that can contribute to antibiotic resistance in *C. difficile* is the extrusion of antimicrobial compounds by efflux pumps. Many of the efflux pumps studied in *C. difficile* to date correspond to the multidrug and toxic compound extrusion (MATE) family and the major facilitator superfamily (MFS) of efflux pumps. A TolC homolog was initially reported by Mukherjee *et. al* in 2002 and also observed in Govind's lab (unpublished). TolC is part of a resistance-nodulation-division (RND) pump complex normally found in gram-negative bacteria. These reports were surprising because TolC is normally expressed in the outer-membrane of gram-negative bacteria and *C. difficile* does not have an outer-membrane.

The presence of a gram-negative efflux pump complex homolog in *C. difficile* is intriguing. The goal of this project was to provide initial insights into the roles and mechanisms of this complex. To do this, a number of experiments were designed to provide information about the structures, localization, and functions of this protein complex. Based on predicted structures, it was determined that CD_AcrA, CD_AcrB, and CD_TolC have striking structural resemblance to *E. coli* AcrA, AcrB, and TolC, respectively. This, in turn, suggests that the

functions and mechanisms of the *C. difficile* efflux pump might be similar to that of the *E. coli* pump. It was determined that acidic pH conditions and a small number of antimicrobials, including inorganic compounds, organic compounds, fungicides, and antibiotics, inhibit growth of a *C. difficile* mutant lacking this pump system. Interestingly, higher NaCl in the medium and alkaline pH seem to promote the growth of a *C. difficile* mutant lacking this pump or, surprisingly, only inhibit growth of the wild type strain. The experiments performed in this project suggest that the CD_AcrA-AcrB-TolC efflux pump might have an essential role in *C. difficile* physiology, possibly by serving as an efflux pump for toxic metabolites.

Table of Contents

List of Figures

List of Tables

Acknowledgements

This thesis would have not been possible without the support and contributions of several people. I would like to thank my committee, Dr. Revathi Govind, Dr. Govindsamy Vediyappan, Dr. Sanjeev Narayanan, and Dr. Thomas Platt. I would also like to thank Dr. Nigel Minton for sharing the plasmid pMTL007C, and Dr. Robert Fagan for providing the plasmid pRPF185. Finally, I would like to thank my current and past lab members for all their help in performing and troubleshooting these experiments, particularly to Brintha Parasumanna Girinathan.

Dedication

This work is dedicated to my parents, Dr. Benjamin Espinola and Lic. Graciela Lopez de Espinola, for all their support and the sacrifices they had to make for me to be where I am today.

Chapter 1 - Introduction

Clostridium difficile

Clostridium difficile, a gram-positive, anaerobic bacterium, is a major cause of antibiotic-related diarrhea and pseudomembraneous colitis. In the last decades, *C. difficile* has emerged as a major threat because of its tendency to cause frequent and severe disease [1]. Pathogenic strains produce two toxins, TcdA and TcdB. These toxins are the major virulence factors. The virulence mechanism involves the disruption of host intestinal epithelial cells by small GTPases of the Rho family in the cells of the host, this leads to disruption of the actin cytoskeleton in those cells [2, 3]. Over the last decade, there has been a significant increase in the incidence of *C. difficile* infection in the United States, Canada, and Europe. Because of the severity of the infection and its high rate of recurrence, there is a significant financial burden on healthcare systems [4].

Antibiotic treatments are a primary risk factor for the development of *C. difficile* infection because they disrupt the normal gut flora in the host, enabling the antibiotic resistant bacterium to colonize the colon [3-5]. *C. difficile*'s adaptability to its environment and genome plasticity had contributed to the emergence of new epidemic strains with one common feature, resistance to multiple antibiotics. Antibiotics such as cephalosporins, clindamycin, and fluoroquinolones have a higher risk of *C. difficile* infection than others [4]. Most of the resistance mechanisms reported to date can be classified as either antibiotic-degrading enzymes or modification of target sites. In addition to that, strains resistant, or less susceptible, to some antibiotics used to treat *C. difficile* infection, like metronidazole, vancomycin, fidaxomicin, and rifamycins, have been reported [4]. Resistance mechanisms to these antibiotics have been poorly characterized.

Another mechanism that can contribute to antibiotic resistance in *C. difficile* is the extrusion of antimicrobial compounds by efflux pumps. One example is the *cdeA* gene from *C. difficile*, which was reported to make *Escherichia coli and Clostridium perfringens* resistant to ethidium bromide and fluoroquinolone [6]. Another example is the Cme pump, which was identified as a homolog to the NorA efflux pump found in *Staphylococcus aureus*, and was shown to confer resistance to ethidium bromide, erythromycin, and other compounds [7]. A third example are the Tet(P) [8] and Tet(40) [9] efflux proteins that confer resistance to tetracycline, and are found in some *Clostridium* species. Efflux pumps are a sophisticated mechanism evolved by bacteria to adapt to the challenges that their niches might present. A brief general review of efflux pumps is given in the following section.

Efflux pumps

Bacterial efflux pumps are involved in antibiotic resistance because of their ability to export a wide range of antimicrobial drugs, both synthetic and natural[10, 11]. There are many families of multidrug transporters, including the multidrug and toxic compound extrusion (MATE), resistance-nodulation-division (RND), small multidrug resistance (SMR), major facilitator superfamily (MFS), and ATP-binding cassette (ABC) transporters. All the families of transporters are found in gram-positive and gram-negative bacteria, except for the RND family, which is only found in gram-negative bacteria [11]. Regarding to the pumps mentioned before, the CdeA pump is a member of the MATE family [6], the Cme and the Tet pumps are members of the MFS family [7-9].

There are clear differences when comparing the transport mechanisms between the different families of transporters, and there are differences when comparing members of the

same family too [10]. One family with particularly complicated mechanism is the RND family. The reason for this complexity is that they are formed by a complex of multiple proteins, which can in turn be decoupled from one another [10]. For example, the AcrAB-TolC is a tripartite complex involved in antibiotic resistance in a number of gram-negative bacteria; TolC, however, can work together with *E. coli*'s EnTS, a MFS protein, to export the siderophore enterobactin outside of the cell [10].

A number of years ago, Dr. Revathi Govind prepared a Western Blot with whole cell lysate samples from *C. difficile*. A graduate student in her lab was put in charge of adding the appropriate antibodies to the blot. Unfortunately, the student added an *E. coli* anti-TolC antibody. Once the blot was developed, it was clear to Dr. Govind that the visible bands were not her bands of interest. To her amazement, it seemed like the anti-TolC antibody was reacting very specifically with a protein present in the *C. difficile* preparation. This was one of the first accounts of the presence of a TolC-like protein in *C. difficile*, or for that matter in a gram-positive bacterium.

The presence of a TolC-like protein in *C. difficile* was also reported by Mukherjee et al. in 2002 [3]. They found a 47 kDa protein in extracellular preparations. This protein matched with an open reading frame in the genome of the CD630 strain encoding a 49 kDa protein (named CD630_24080), and it had weak C-terminus homology with TolC and with other efflux proteins of gram-negative bacteria. Interestingly, they reported that the extracellular concentration of the 47 kDa protein increased up to 10 times in high toxin production conditions. A second, more recent report of an outer-membrane protein in *C. difficile* was published in 2012 by Boetzkes et al. [12]. In that study, they identified a 49.5 kDa protein in *C. difficile* R20291 culture supernatant. This protein was identified as CDR20291_2298, which has 99% sequence

homology to the extracellular protein identified by Mukherjee et al. These two reports comprise most, if not all, of the published information of a TolC-like protein in *C. difficile*. The presence of a gram-negative outer membrane protein homolog in a gram-positive bacterium is intriguing. In this study, we hypothesized that this TolC-like protein is part of a novel type of transporter and designed experiments to characterize this unique protein in *C. difficile*.

In the CD630 genome, the TolC homolog is coded in the ORF CD630_24080, which is part of an operon that carries ORFs CD630_24060 and CD630_24070. In the CDR20291 genome, the operon comprises of ORFs CDR20291_2296, CDR20291_2297, and CDR20291_2298. **Figure 1.1** shows the locus in the CD630 genome, with the three genes highlighted in a box.

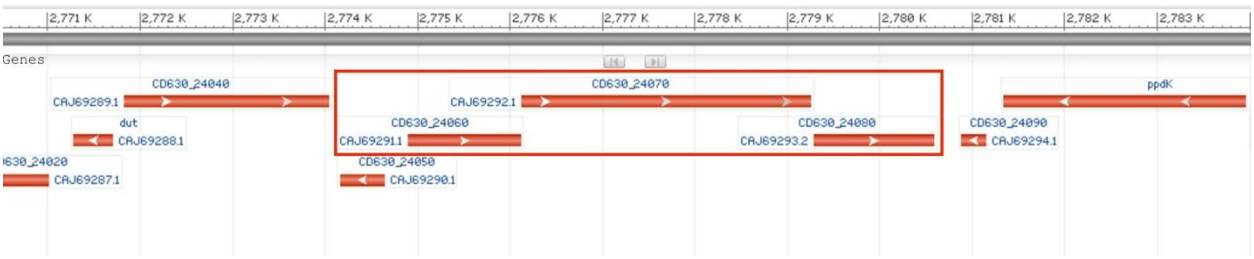

Figure 1.1 - Genome organization

GenBank image of the locus where the open reading frame identified by Mukherjee *et al.* is found. This ORF, along with the two ORFs with weak homology to AcrA and AcrB, are highlighted in a box.

In silico analyses of this region using fgenesB operon prediction further supported that these three ORFs are indeed part of an operon. In **Figure 1.2**, the three genes in question are highlighted in a box. The genes were predicted to be part of an operon, and the genes downstream and upstream of the locus were predicted to be transcription units, i.e. not part of an operon. It is important to note that analyzing the locus in question alone or together with many more genes does not change the results. Additionally, BLAST analysis of CD630_24060 and

CD630_24070 revealed that the proteins coded have weak homology to AcrA and AcrB in *E. coli*, respectively. These results strengthen the possibility that the proteins coded in this operon are related to the AcrAB-TolC RND efflux pump found in *E. coli* and other gram-negative bacteria.

```
Length of sequence - 12500 bp
Number of predicted genes - 6
Number of transcription units - 4, operons - 1
    N      Tu/Op   Conserved  S             Start          End    Score
                   pairs(N/Pv)
    1     1 Tu  1      .       +    CDS        173 -      2401   1425
    2     2 Tu  1      .       -    CDS       2512 -      2997    324
    3     3 Op  1      .       +    CDS       3276 -      4472   1030
    4     3 Op  2      .       +    CDS       4476 -      7610   2345
    5     3 Op  3      .       +    CDS       7632 -      8942   1181
    6     4 Tu  1      .       -    CDS       9690 -     12317   2106
```

Figure 1.2 - fgenesB operon prediction

Results of operon prediction analysis of the locus presented above. N 3, 4, 5 (highlighted in a box) correspond to the AcrA, AcrB, TolC homologs, respectively.

As mentioned before, there have not been any reports of any RND efflux pumps in gram-positive bacteria. However, studies done in gram-negative bacteria could provide insights into the functions that this complex has. In gram-negative bacteria, TolC can function with several protein complexes. One of the best characterized complexes is the AcrAB-TolC multidrug efflux pump, which will be reviewed in the following section.

AcrAB-TolC

E. coli's acridine resistance complex, AcrAB-TolC complex, is the best characterized RND transporter [10, 13]. This tripartite complex is composed of an inner-membrane transporter AcrB, an outer-membrane channel TolC, and a periplasmic protein AcrA. **Figure 1.3** shows the most common representation of the complex in published studies. The AcrAB-TolC complex can

transport a very wide range of small molecules. Interestingly, the substrates for the complex share little structural or chemical similarity. Some of those substrates include: erythromycin, , novobiocin, bile salts, and β-lactam antibiotics [10]. Homologs of this complex have been reported in other organisms. For example, *Salmonella typhimurium* has a similar system, also called AcrAB-TolC, with similar substrate preferences [14]. *Pseudomonas aeruginosa* has a homolog complex too, the MexAB-OprM complex, with similar export capabilities as the *E. coli* counterpart [15].

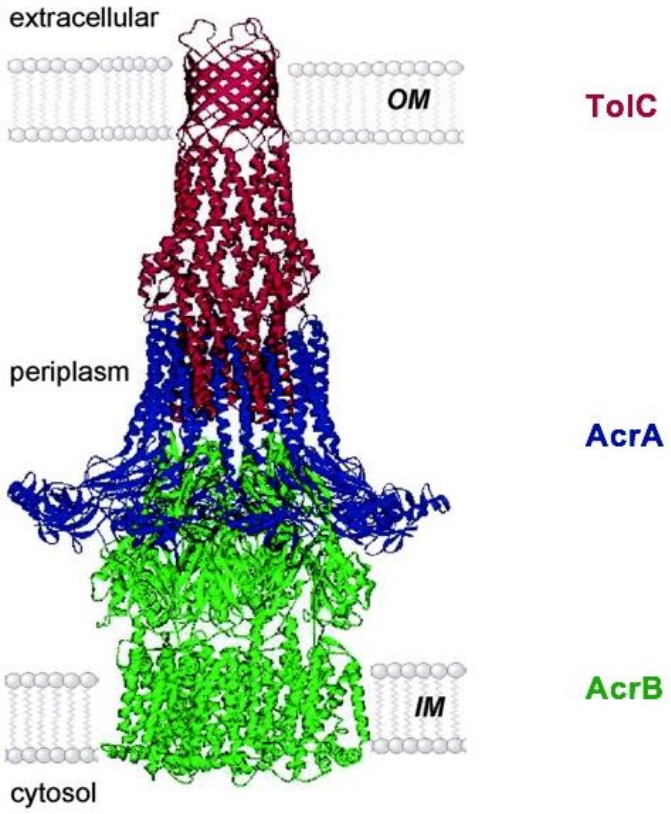

Figure 1.3 - AcrAB-TolC structure
Model of the assembled complex published by Eswaran *et al.* [16].

The complex is thought to be associated in a 3:6:3 AcrB:AcrA:TolC ratio. This ratio has been seen in cryo-EM representations and observed in previously published studies [17].

Interestingly, the cryo-EM representations show that there is no direct interaction between AcrB and TolC. The representations show a large channel stretching from the outer-membrane to the inner-membrane, where TolC is the outer-membrane component and AcrB is the inner-membrane component, and both are bridged by AcrA [10]. Additionally, TolC assumes a constant closed state *in vitro*; however, this conformation changes to an open state upon interaction with AcrA [10]. The current model for drug export by AcrB is a three-step functional rotation mechanism, proposed by Murakami et al. in 2006 [18] and confirmed by other groups [19, 20]. In the first step, the loose state, a substrate can access the binding pocket from the cytoplasmic side of the complex. In the second step, the binding step, the binding pocket expands to allow the substrate to bind to bind the different sites in the pocket. In the final step, the extrusion state, the bound substrate is pushed out of the binding pocket.

Antimicrobial export might not be the only function of AcrAB-TolC and other efflux pump complexes. It has been proposed that efflux pumps have physiological functions too, including stress adaptation, development, and pathogenesis [11]. In *E. coli*, AcrAB-TolC is able to pump bile salts out of the bacteria [21]. Bile salts are toxic to many enteric bacteria, including *E. coli*, as they disrupt cell membranes. Therefore, AcrAB-TolC functioning as a bile salt pump contributes to the adaptation to the intestinal tract. Evidence for similar functions in other bacteria expressing AcrAB-TolC homologs has been reported for *S. Typhimurium* [22], *Neisseria gonorrhoeae* [23], and *P. aeruginosa* [24]. AcrAB-TolC systems could also have a direct role in bacterial pathogenesis. By testing the ability of *P. aeruginosa* to invade Madin-Darby canine kidney (MDCK) cells, a type of epithelial cells, Hirakata *et al.* showed that mutants lacking the MexAB-OprM system could not invade MDCK cells [25].

Another proposed role of AcrAB-TolC homologs in bacterial adaptation is cell-to-cell communication through quorum sensing. Quorum sensing responses are dependent on the release of chemical signals called autoinducers, which are released as a function of population density. Once the autoinducers reach a minimum threshold concentration, cellular functions can be altered. An efflux pump involved in quorum sensing was first reported in *P. aeruginosa [11]*. It was reported that strains overexpressing the MexAB-OprM efflux complex led to reduced production of autoinducers and, therefore, reduced quorum sensing response [26]. Later, it was reported that lack of the MexAB-OprM system in *P. aeruginosa* led to reduced diffusion of autoinducers and increased intracellular concentrations of autoinducers [27]. The connection of efflux pumps with quorum sensing has been observed in *E. coli* too. Rahmati *et al*. reported that the overexpression of a quorum sensing regulator, SdiA, led to increased expression of AcrA and AcrB [28], suggesting the involvement of the AcrAB system in quorum sensing.

Another proposed role of AcrAB-TolC homologs, and other efflux pumps, is the formation of biofilms, a characteristic of chronic bacterial infections [11]. Kvist *et al.* reported that biofilm formation is abolished by the use of efflux pump inactivators in *E. coli* and *Klebsiella pneumoniae* [29]. More recently, it was reported that *E. coli* strains lacking AcrA or AcrB had reduced biofilm formation [30]. The same study showed that other efflux pumps had reduced, and some abolished, biofilm formation too. Similarly, in it was reported that *S. typhimurium* lacking any efflux pumps, including AcrAB-TolC, results in abolished biofilm formation [31].

Research Objectives

The AcrAB-TolC efflux pump has a variety of roles in gram-negative bacteria. These roles, however, occur under the assumption that the efflux pump complex conforms to the standard localization, an inner-membrane AcrB and an outer-membrane TolC, both bridged by the periplasmic protein AcrA. *C. difficile* is a gram-positive bacterium, therefore, the cellular membrane is significantly different from that of the gram-negative species that express AcrAB-TolC or homologs. What kind of functions could an efflux pump complex like AcrAB-TolC have in a gram-positive bacterium? How are the proteins organized in the membrane? Do they exist in a tripartite conformation like in *E. coli*? Are there any structural features conserved despite the sequence disparities? The goal of this project is to explore some of these questions. The specific goals of this project are divided in three parts: to determine the structure of the three proteins, to determine their localization, and to characterize their functions.

In this project, two strains of *C. difficile* will be studied: JIR8094 and R20291. Throughout this project, the JIR8094 strain will be also referred to as J strain. Similarly, the R20291 strain will be referred to as R strain. The three proteins of interest, although sharing great sequence similarity, have been annotated with different names in the two genome databases. Therefore, a renaming is necessary for the purposes of simplicity and clarity. For both strains, the first gene in the operon will be referred to as CD_*acrA*, the second gene as CD_*acrB*, and the third gene as CD_*tolC*. Proteins will be named in a similar fashion.

Chapter 2 - Experimental Procedures

Bacterial Growth Conditions

C. difficile strains (**Table A.1**) were grown anaerobically (10% H_2, 10% CO_2, and 80% N_2) in tryptose-yeast extract (TY) broth or TY agar plates [32-34], and *C. difficile* mutant strains (**Table A.1**) were grown in the same conditions but with addition of lincomycin (20 µg/mL). E. coli strains, S17 and DH5α (see **Table A.1**), were grown aerobically in LB broth or agar plates supplemented with chloramphenicol (30 µg/mL) or ampicillin (100 µg/mL) when needed. All routine cloning and plasmid construction were carried out using standard procedures (**Table A.2**). Oligonucleotides used in this study can be found in **Table A.3**.

Preparation of Membrane Protein Samples

Separation of membrane proteins from cytosolic proteins was done as previously described [35]. Cells were harvested by centrifugation, resuspended in Tris buffer (50 mM Tris-HCl, pH 7.5), and disrupted by passage through a French pressure cell. The disrupted cells were incubated in Benzonase nuclease (Sigma-Aldrich) for 30 minutes at 4°C. Unbroken cells were removed by centrifugation at 3,000*g* for 20 minutes at 4°C. The supernatant was centrifuged at 245,000*g* for 120 minutes at 4°C to separate the cytosolic proteins (in the supernatant) from the membrane and cell wall-associated proteins (in the pellet). To further separate membrane proteins from cell wall-associated proteins, the pellet was resuspended in Tris buffer with 1% n-Dodecyl-β-D-maltoside (DDM) for 8 hours at 4°C. Following centrifugation at 16,000*g* for 30 minutes, the resulting supernatant contains the soluble membrane proteins, and the pellet contains the cell wall-associated proteins.

Purification of CD_TolC

A pJ401 vector carrying CD_*tolC* (pRGL66 in **Table A.2**) with codons optimized for expression in *E. coli [36]*, a six carboxy-terminal histidine tag, and an inducible promoter was synthesized by ATUM (Newark, CA). The cloned gene was expressed in *E. coli* Rosetta competent cells (DE3) and induced overnight at 4°C with 1 mM IPTG after an initial 4-hour growth at 37°C. Total membrane proteins were extracted as described above. The overexpressed CD_TolC was purified using a Ni^{2+} beads (Sigma-Aldrich). The affinity-purified protein was then separated from the beads with imidazole and verified by Western blot analysis and CBB staining.

Creation of TolC-specific Antibodies

A rabbit was used to raise CD_TolC-specific antibodies with the purified protein. Immunizations and blood collections were carried out by Lampire Biological Laboratories, Inc. (Pipersville, PA). CD_TolC-specific antibodies were enriched after preadsorbing the collected serum against purified CD_TolC protein.

Construction of Mutants

C. difficile strains ΔCD_*acrA*, ΔCD_*acrB*, and ΔCD_*tolC* in both the J and R backgrounds were generated by insertion of a bacterial group II intron using the ClosTron gene system [37]. The introns were designed using web-based Perutka algorithm [38] design tool, available on the ClosTron website (http://clostron.com). They were then synthesized and cloned into the vector pMTL007C-E5 by ATUM (Newark, CA). In this fashion, plasmids pRGL49, pRGL89, pRGL362, pRGL363 were generated (**Table A.2**). The synthesized plasmids were

transferred to *C. difficile* by conjugation as described previously [37, 39]. Thiamphenicol-resistant transconjugants were transferred to TY agar plates supplemented with lincomycin to select for potential mutants, since successful insertion of the intron into the target gene confers lincomycin resistance. The selected lincomycin resistant mutants were screened by PCR as described in **Chapter 3**.

Western Blot Analyses

Sample proteins were collected, separated by SDS-PAGE, and immobilized onto polyvinylidene difluoride (PVDF) membranes suing the semi-dry blot technique using the Tans-Blot SD Transfer Cell (Bio-Rad Laboratories, Inc.). Membranes probed with anti-CD_TolC antibodies used a 1:1,000 antibody:buffer dilution followed by horseradish peroxidase-conjugated anti-rabbit secondary antibodies. Membranes probed with anti-6-His tag antibodies used a 1:10,000 antibody:buffer dilution. Note that this antibody is HRP conjugated.

Complementation of *C. difficile* ΔCD_*acrA-acrB-tolC* with CD_*tolC*

The CD_*tolC* ORF along with its ribosomal binding site were PCR amplified using the chromosomal DNA of the JIR8094 strain using primers ORG570 and ORG683 (**Table A.3**). The resulting PCR product was cloned into the pGEM-T Easy vector. Multiple plasmids were sequenced by Genewiz (South Plainfield, NJ), and a plasmid with correct insert was selected, pRGL364 (**Table A.2**), and then digested with SacI and BamHI and cloned into vector pRPF185 (**Table A.2**) under a tetracycline-inducible promoter. Multiple plasmids were sequenced by Genewiz (South Plainfield, NJ) and a plasmid with correct insert was selected, pRGL365 (**Table A.2**). The plasmid was then introduced into the JΔCD_*acrA-acrB-tolC* strain by conjugation

[39]. Transconjugants carrying pRGL365 or the vector control (pRPF185) were grown overnight at 37°C in TY broth supplemented with thiamphenicol. Fresh 10mL cultures were initiated using 100µL of overnight culture and grown for two hours at 37°C in TY broth supplemented with thiamphenicol. Then induction with 100ng/mL of ATc (anhydrotetracycline) was done. Cultures were harvested 10 hours after induction.

Extraction of Surface-layer Proteins

Surface-layer proteins (SLPs) were extracted using 0.2 M glycine pH 2.2 as described previously [40, 41]. 50 mL of exponential phase culture were harvested by centrifugation (3000*g* for 20 minutes at 4°C), washed twice in phosphate-buffered saline (PBS), resuspended in 200 µL of 0.2 M glycine pH 2.2, and incubated at room temperature for 30 minutes. Then, the cell pellet was removed by centrifugation (16,000*g* for 15 minutes at 4°C). The resulting supernatant, which contained the SLPs, was dialyzed into 10 volumes of PBS using a 3 kDa MW-cutoff dialysis bag, and pre-reduced before use.

Microscopy

Cell cultures were grown as required in appropriate medium. Cell samples were harvested by centrifugation. The samples were chemically fixed by resuspending the pellets in 2% paraformaldehyde for 30 minutes at room temperature. The fixed cells were washed at least three times in PBS. All prior steps were carried out under anaerobic conditions. The samples were diluted in PBS and observed with a phase-contrast microscope (Zeiss LSM5 Pascal).

Construction of Growth Curves

The growth patterns of the different mutants were studied in different medium conditions. Initially, overnight cultures were grown in TY medium supplemented with appropriate antibiotics. Fresh 100mL cultures were initiated using 1mL of overnight culture and grown at 37°C in the appropriate medium. Three samples from each culture were taken at the different time points, and the OD_{600} was recorded. Experiments were done with at least three biological replicates.

Sporulation Quantification

Cells were streaked in fresh TY agar plates supplemented with the appropriate antibiotics and grown at 37°C for different lengths of time. Samples were collected and resuspended in PBS buffer for phase-contrast microscopy as described previously [42-44]. At least five fields per strain and condition were obtained, and the number of spores and vegetative cells was counted.

PM Assays

Phenotype Microarray assays were done using PM plates (Biolog) following the manufacturer's indications and previously published studies [45]. The strains to be analyzed were grown overnight at 37°C in TY medium. Cell pellets were harvested by centrifugation at 3000*g* for 10 minutes at 4°C and resuspended in IF-0a inoculating fluid (Biolog). The bacterial suspension was adjusted until a transmittance of 40% was obtained. The suspension was further diluted 1:16 in IF-0a (for the osmolytes and pH plates) or IF10b (for the chemical sensitivity plates). Plates were then inoculated with 100 µL per well and incubated at 37°C for 18 hours. OD_{600} was then recorded. All PM plates and inoculating fluids were converted to an anaerobic

state by deoxygenation with Pack-Anaero oxygen absorbers (Mitsubishi). The IF-0a inoculating fluid was supplemented with 12 mM sodium bicarbonate and 480 µM sodium thioglycolate, as indicated by the manufacturer.

ICP-OES

To measure intracellular sodium ion concentrations, inductively coupled plasma optical emission spectroscopy (ICP-OES) was used. Cells were grown overnight at 37°C in TY broth supplemented with appropriate antibiotics. Fresh 10mL cultures were initiated using 100µL of overnight culture and grown for 12 hours at 37°C in TY broth. Cell pellets were harvested by centrifugation (3,000*g* for 20 minutes at 4°C), resuspended in 70% nitric acid, and incubated overnight at room temperature. Dissolved samples were diluted to obtain a final 4% acid content. Samples were then analyzed in a Varian 720-ES ICP-OES instrument. At least three biological replicates were used.

Statistical Analyses

Significance was determined using analysis of variance (ANOVA) to enable comparison between multiple groups. The Least Significant Different (LSD) test was used for posthoc analyses. P values of statistically significant differences are shown as one star ($p<0.05$) or two stars ($p<0.01$). All graphs include error bars, which represent standard deviation.

Chapter 3 - Results

Structure

E. coli Anti-TolC antibodies reacting specifically against a *C. difficile* protein suggested the existence of a *C. difficile* protein that shares structural similarity to *E. coli's* TolC. Mukherjee *et al.* identified a protein with weak homology to TolC [3]. As mentioned in **Chapter 1**, that protein shares little to no amino acid or nucleotide sequence similarity with *E. coli* TolC. This could mean that Dr. Govind's serendipitous observation and the later reports by Mukherjee *et al.* and Boetzkes *et al.* are not about the same protein.

As an initial step, the amino acid sequences of CD_*tolC* and the two proteins that are part of the operon, CD_*acrA* and CD_*acrB*, were sent to the I-TASSER on-line server (http://zhanglab.ccmb.med.umich.edu/I-TASSER/) for structure and function prediction. **Figure 3.1** shows the structure predictions for CD_AcrA (**A**), CD_AcrB (**B**), and CD_TolC (**C**) based on JIR8094 amino acid sequences and CD_AcrA (**D**), CD_AcrB (**E**), and CD_TolC (**F**) based on R20291 amino acid sequences. The models shown correspond to the models with the higher C-scores, which represent the model with the highest level of confidence as determined by I-TASSER. Although the amino acid sequences of JIR8094 (**Figure 3.1**, panels **A**, **B**, and **C**) and R20291(**Figure 3.1**, panels **D**, **E**, **F**) have few sequence differences, the predicted structures are close to identical.

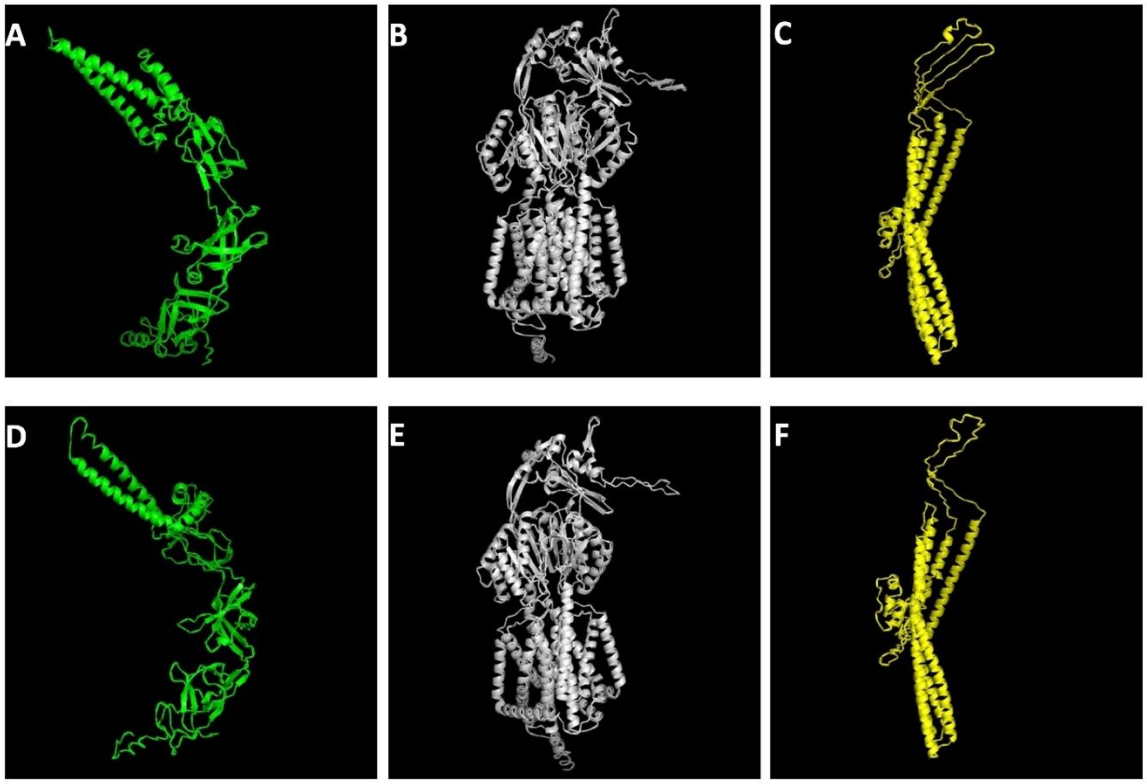

Figure 3.1 - I-TASSER predicted structures based on *C. difficile* sequences

Models determined by the I-TASSER online served for the CD630 protein sequences of: (A) CD_AcrA, (B) CD_AcrB, (C) CD_TolC; and models determined for the R20291 protein sequences of: (D) CD_AcrA, (E) CD_AcrB, (F) CD_TolC.

A feature of I-TASSER is that proteins in the Protein Data Bank (PDB) that are structurally similar to the predicted models are identified automatically. For the predicted structure of CD_TolC, the closest structural analog identified was *E. coli*'s TolC (PDB ID: 1TQQ). For the predicted structure of CD_AcrB, the closest structural analog identified was *E. coli*'s AcrB (PDB ID: 3D9B). For the predicted structure of CD_AcrA, the closest structural analog identified was the ZneB (PDB ID: 3LNN) protein from *Cupriavidus metallidurans*; *E. coli*'s AcrA (PDB ID: 2F1M) was the fifth closest structural analog. **Figure 3.2** shows the predicted structures of CD_AcrA (A), CD_AcrB (B), and CD_TolC (C) based on the J8094 sequences superimposed to their *E. coli* counterparts. The resemblance to the *E. coli* counterparts is striking considering that there is little to no nucleotide or amino acid sequence similarity.

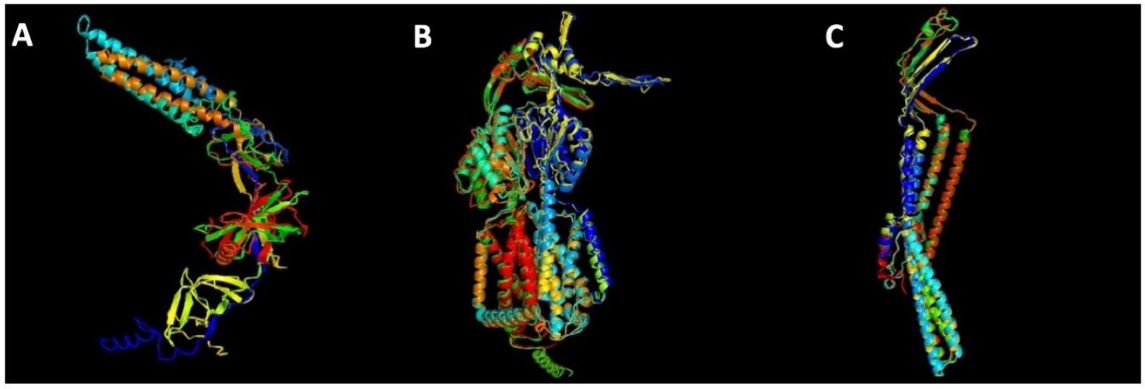

Figure 3.2 - Comparison of predicted models to published crystal structures

Predicted models based on the CD630 sequences of (A) CD_AcrA, (B) CD_AcrB, (C) CD_TolC superimposed to published crystal structures of *E. coli* AcrA (PDB ID: 2F1M), AcrB (PDB ID: 3D9B), and TolC (PDB ID: 1TQQ), respectively.

Because of the great structure similarities between the predicted structures of CD_AcrA, CD_AcrB, and CD_TolC and their *E. coli* counterparts, it seemed essential to obtain crystal structures of CD_AcrA, CD_AcrB, and CD_TolC to confirm this observation. Plasmids carrying CD_*acrA*, CD_*acrB*, or CD_*tolC* with codons optimized for expression in *E. coli* [36] and purification tags were synthesized by ATUM (Newark, CA). pRGL69 expresses CD_*acrA* with a FLAG-tag, pRGL70 expresses CD_*acrB* with a Step-tag, and pRGL66 expresses CD_*tolC* with a polyhistidine-tag. Unfortunately, not enough protein with sufficient purity for X-ray crystallography was obtained. However, it was possible to purify enough CD_TolC to raise antibodies against it. The antibodies were tested and enriched as described in **Chapter 2**. It was found that the anti-CD_TolC antibody provided great reactivity and specificity to recombinant CD_TolC expressed in *E. coli* and *C. difficile*.

Mutagenesis to disrupt CD_*acrA*, CD_*acrB*, and CD_*tolC* in *C. difficile*

The predicted structures seem to indicate that CD_AcrA, CD_AcrB, and CD_TolC could be analogs of the AcrAB-TolC pump of gram-negative bacteria, therefore, additional studies

were pursued to attempt to characterize their functions and mechanisms. As an initial step, mutant strains were generated with the ClosTron mutagenesis method as described in **Chapter 2**. **Figure 3.3** and **Figure 3.4** show the PCR products obtained with different primer combinations. In each pane, lane one corresponds to the DNA ladder, lane two is the PCR product obtained with gene specific primers using genomic DNA form the parent strain as a template, lane three is the PCR product obtained with gene specific primers using genomic DNA form the mutant candidate as a template, lane four is the product of the EBS Universal primer and the gene specific forward primer, and lane five is the product of the EBS Universal primer and the gene specific reverse primer (see **Table A.3** for oligonucleotides used in this experiment). A larger PCR product in lane 3, compared to lane 2, proves insertion of the intron into the target in the genome. A product in lane 4 and no product in lane 5 shows proper orientation of the intron. **Figure 3.3** shows successful creation of three mutants in the J background, JΔCD_*acrA*, JΔCD_*acrB*, and JΔCD_*tolC*. **Figure 3.4** shows successful creation of two mutants in the R background, RΔCD_*acrA* and RΔCD_*tolC*. Unfortunately, an RΔCD_*acrB* strain was not obtained to date.

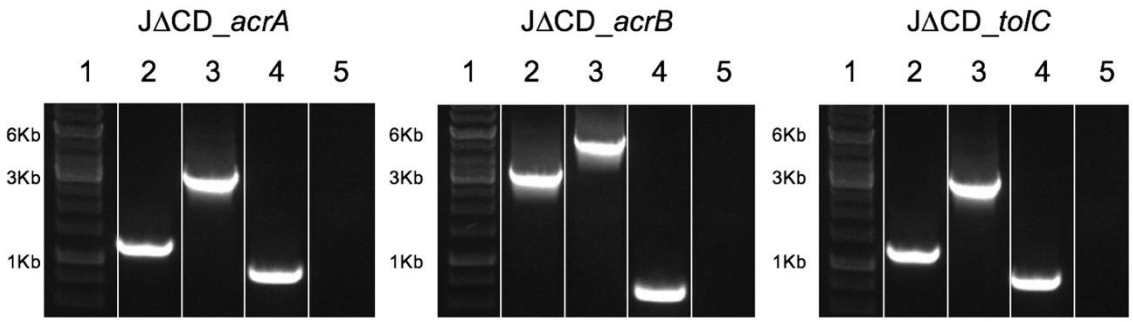

Figure 3.3 - PCR analysis of recombinant J strains

Each pane corresponds to a different targeted gene. Lanes 2 and 3 show the products of gene specific primers using the parent genomic DNA and mutant genomic DNA, respectively. Lanes 4 and 5 show the product obtained using the EBS Universal primer and forward gene specific primer (4) or reverse gene specific primer (5).

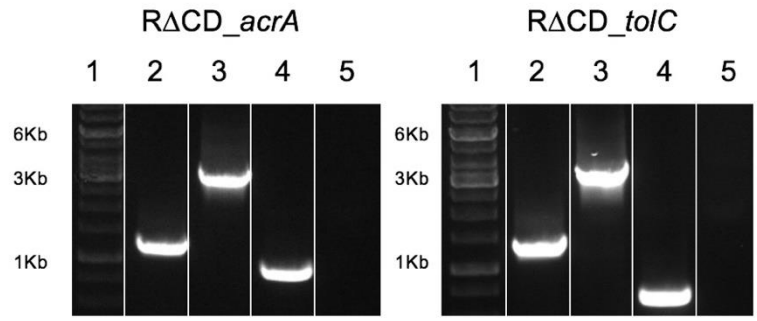

Figure 3.4 - PCR analysis of recombinant R strains

Each pane corresponds to a different targeted gene. Lanes 2 and 3 show the products of gene specific primers using the parent genomic DNA and mutant genomic DNA, respectively. Lanes 4 and 5 show the product obtained using the EBS Universal primer and forward gene specific primer (4) or reverse gene specific primer (5).

As mentioned in **Chapter 1**, *in silico* analysis suggests that CD_*acrA*, CD_*acrB*, and CD_*tolC* are transcribed as an operon. If that is the case, then an insertion mutation disrupting the first gene of the operon would disrupt the reading frame of the genes downstream, generating a triple mutant, e.g. the ΔCD_*acrA* strain described above is a ΔCD_*acrA-acrB-tolC* strain, and similarly a mutation in the second gene generates a double mutant. Therefore, a strain in which the gene CD_*acrA* was targeted by ClosTron mutagenesis will be referred to as ΔCD_*acrA-acrB-tolC*, a strain in which the gene CD_*acrB* was targeted will be referred to as ΔCD_*acrB-tolC*, and a strain in which the gene CD_*tolC* was targeted will be referred to as ΔCD_*tolC*.

Localization of CD_TolC in *C. difficile*

The anti-CD_TolC antibody was used to attempt to localize CD_TolC expressed natively in *C. difficile*. Previous RT-PCR experiments indicate that CD_TolC is expressed at maximum levels after 12 hours of culture in TY medium (**Figure B.2**). Cell samples of the different J and R stains were collected at that time point. Cells were processed to fractionate the cytosolic content and the membrane content, as described in **Chapter 2**. Then Western blotting experiments were

done to detect the presence of CD_TolC. **Figure 3.5** shows the Western blot of the soluble membrane fractions of the different strains, which is the only fraction in which this protein was detected. CD_TolC was detected in the J (lane 1) and R (lane 5) soluble membrane fractions, suggesting that it is localized in the membrane. Note that CD_TolC was not detected in any of the mutants. In the case of the triple and double mutants, this result supports that CD_*acrA*, CD_*acrB*, and CD_tolC are transcribed as an operon since the ClosTron mutagenesis disrupted only the first gene in the operon and left the last gene, CD_TolC, intact. **Figure 3.5** also shows the JΔCD_*acrA-acrB-tolC* strain complemented with the pRPF185 vector carrying CD_TolC (pRGL365, **Table A.2** - Plasmids) in lane 8. The cells were induced with 100ng ATc/mL of culture for 12 hours. Interestingly, under this induction condition, two bands can be observed. The lower band resembles in size to that found in the two parent strains, and the top band resembles the predicted protein size before any post-translational processing.

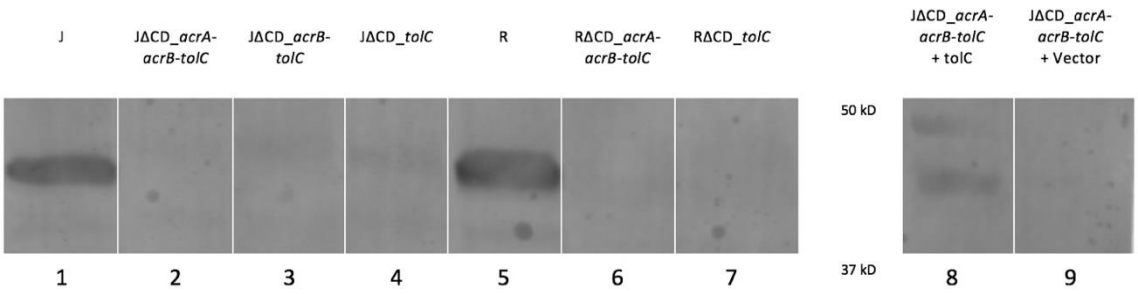

Figure 3.5 - Western blot analysis of the membrane fractions

Western blot analysis showing localization of CD_TolC in membrane fractions. Lanes 1–4 correspond to the J strains, lanes 5–7 correspond to the R strains, lane 8 correspond to the J triple mutant complemented with pRGL365, and lane 9 is a negative control.

In *E. coli*'s AcrAB-TolC complex, TolC is localized in the outer- membrane. If CD_AcrA, CD_AcrB, and CD_TolC follow the same organization, then CD_TolC, in *C. difficile*, would be localized in the peptidoglycan layer and possibly exposed to the surface. To explore this option, surface-layer proteins (SLPs) and cell wall associated proteins from the

parent and mutant strains in the J background were extracted as described in **Chapter 2**. Western blotting using the anti-CD_TolC antibody was done to test for the presence of CD_TolC. As seen in **Figure 3.6**, CD_TolC can be detected in the SLPs preparation of the parent J strain and is absent in the mutant strains., indicating that CD_TolC is a cell wall associated protein in *C. difficile*.

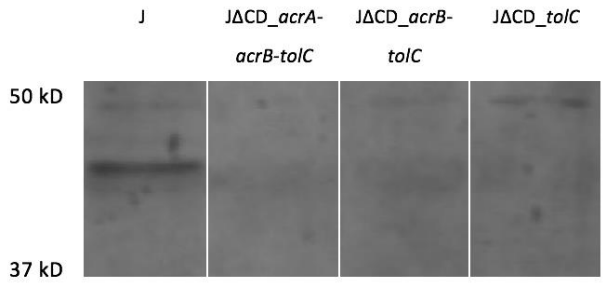

Figure 3.6 - Western blot analysis of the extracted surface-layer proteins
Western analysis using CD_TolC antibody of surface-layer and cell wall proteins extracted from the J strains.

Phenotyping

From the I-TASSER analyses (**Figure 3.2**), it is apparent that CD_AcrA, CD_AcrB, and CD_TolC are structurally similar to *E. coli* AcrAB-TolC. Additionally, cross reactivity of CD_TolC antibody with *E. coli* TolC and vice versa indicate that their adopted conformation is also similar. This information, however, does not give many clues about the functions that this protein complex has in *C. difficile.* To determine their possible roles in *C. difficile,* various phenotypic assays were performed.

Construction of Growth Curves

As a first step, the effect of mutations in CD_*acrA*, CD_*acrB*, or CD_*tolC* on the growth of *C. difficile* was assessed in two different media (**Chapter 2**). **Figure 3.7** shows the growth

curve of the parent and mutant strains in both the J and R backgrounds in TY medium. No significant difference in growth was observed in the R strains (**Figure 3.7 B**). In the J strains (**Figure 3.7 A**), growth was unchanged too, except for the JΔCD_*tolC*, which showed a decrease in turbidity at the start of the stationary phase (at about 12 hours post inoculation).

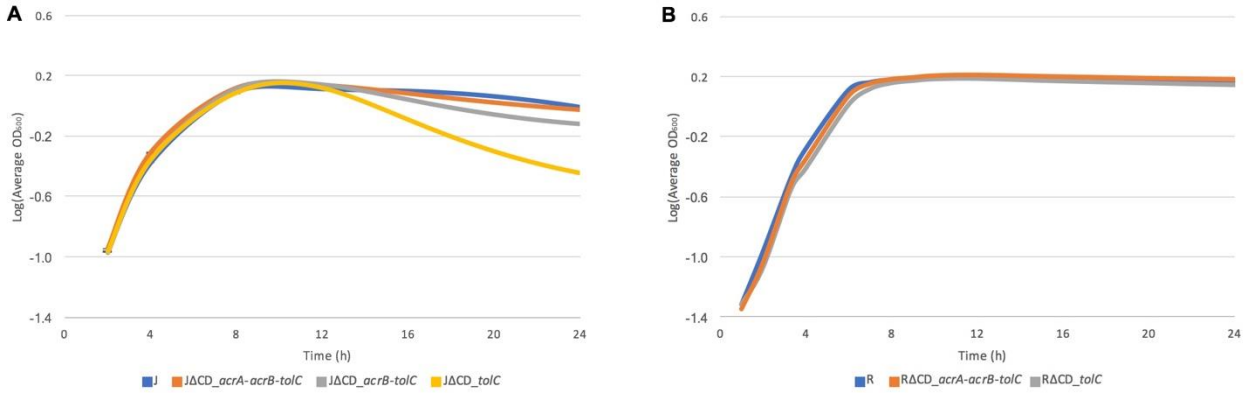

Figure 3.7 - J and R strains grown in TY medium

Growth curves of *C. difficile* strains (A) J and (B) R grown anaerobically in TY medium. The values shown correspond to the log of the average OD_{600} at different time points.

The observations above were consistent in TY medium supplemented with cefoxitin (**Figure 3.8**). The antibiotic cefoxitin belongs to the beta-lactam antibiotic family, which bind to penicillin binding proteins. Cefoxitin does not inhibit *C. difficile* growth; however, it blocks spore formation, possibly by binding to SpoVD, a penicillin binding proteins that is essential for sporulation.

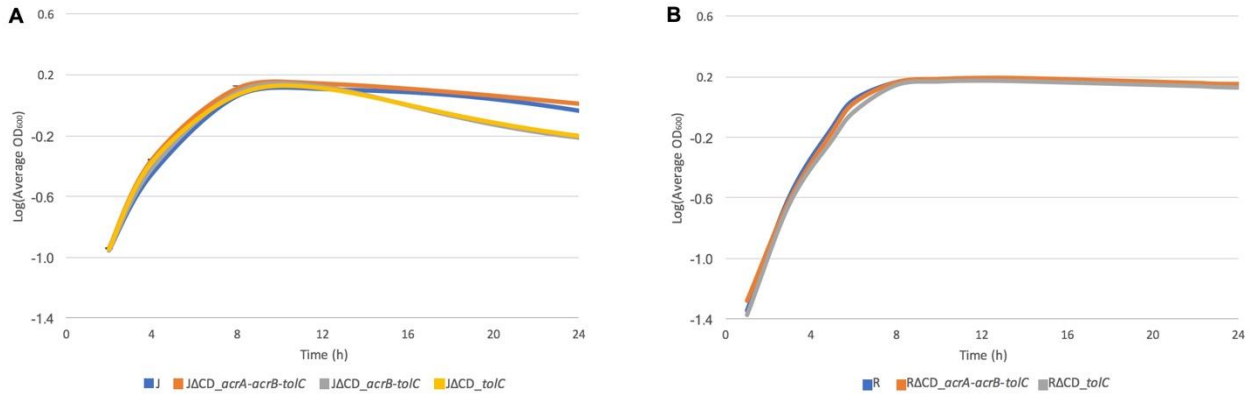

Figure 3.8 - J and R strains grown in TY medium supplemented with Cefoxitin

Growth curves of *C. difficile* strains (A) J and (B) R grown anaerobically in TY medium supplemented with cefoxitin. The values shown correspond to the log of the average OD_{600} at different time points.

Sporulation

Next, the sporulation phenotypes of the parent and mutant strains were studied. Initially, microscopy observations suggested that there is a larger number of spores, seen as bright dots in the images, formed in medium lacking antibiotics in the different mutant strains (**Figure 3.9**). Sporulation is generally upregulated in the presence of adverse environmental conditions. This could indicate that the mutants are unable to import necessary substrates, or, alternatively, to export toxic substrates as a consequence of the absence of CD_AcrA, CD_AcrB, and CD_TolC, or, more indirectly, by upregulation or downregulation of other metabolic pathways. In the presence of cefoxitin there is a different growth phenotype. As seen in **Figure 3.10**, the R mutant strains have a high number of morphological deformations (shown by white arrows). This result seems to indicate accumulation of substrates or failure to control osmoregulation properly. Interestingly, a small number of spores (shown by red arrows) were observed in the R mutants. This is surprising because cefoxitin is able to abolish spore formation in the parent strains. For the J mutant strains, a smaller number of morphological deformations are observed and no spores were observed.

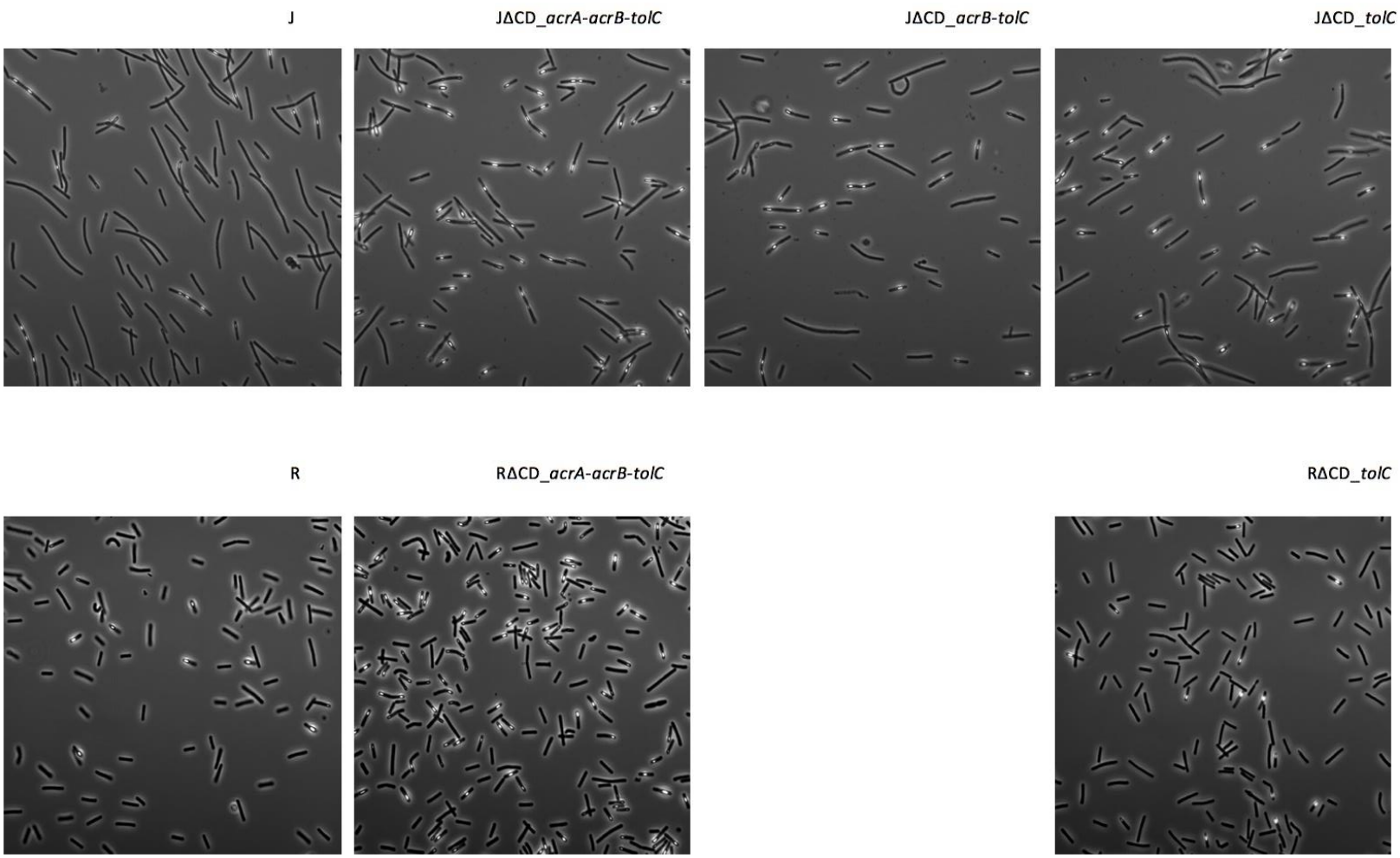

Figure 3.9 - Images of the J and R strains in TY medium

Phase-contrast images of the J strains (left) and R strains (right) after 24 hours of growth in TY plates. The bright white dots are spores.

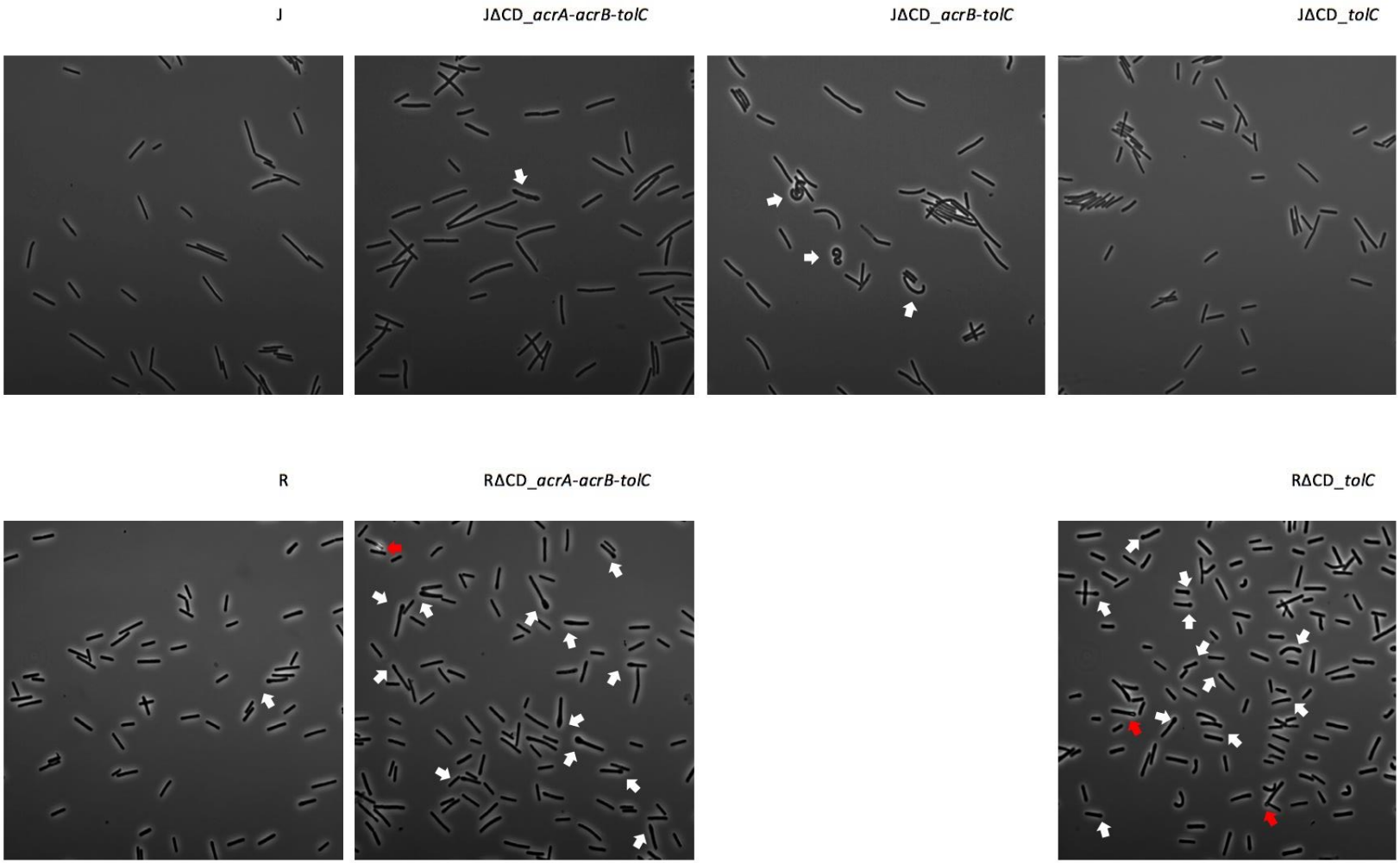

Figure 3.10 - Images of the J and R strains growth in medium supplemented with cefoxitin

Phase-contrast images of the J strains (left) and R strains (right) after 24 hours of growth in TY plates supplemented with cefoxitin. White arrows show morphological abnormalities and red arrows show spores (bright white dots).

Because the change in sporulation was such a striking phenotype in the mutants, quantifying the spores in TY medium was attempted. **Figure 3.11** shows the percentage of spores formed after different lengths of incubation in the different R strains. The number of spores in the RΔCD_*acrA-acrB-tolC* was more than 5 times greater than the parent strain. Similarly, the number of spores in the RΔCD_*tolC* was about 4 times greater than the parent strain. Although this quantification was not done for the J strains, microscopy observations confirm a similar sporulation pattern, the mutant strains produce more spores than the parent.

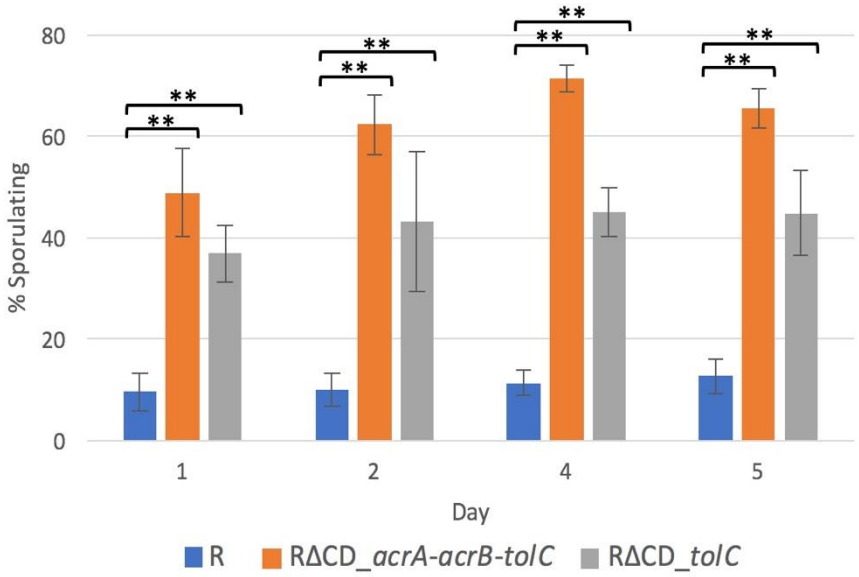

Figure 3.11 - Sporulation efficiency of the R strains

Spore counts of the R strains grown anaerobically in TY plates. The values shown correspond to the average spore:vegetative cell ratio of five fields.

PM Assays

Due to the large number of functions that an AcrAB-TolC analog could have in *C. difficile*, it was considered appropriate to use Biolog's Phenotype Microarray assays (PM assays) to screen for differences in the response to antimicrobial agents and metabolites by measuring cell growth. The PM assays allow the simultaneous screening of hundreds of chemicals in at

least four increasing doses of the test conditions at a time. The experiments were performed using the parent R and the RΔCD_*acrA-acrB-tolC* strains as described in **Chapter 2**. The experiment was carried out using the medium supplied by the manufacturer and the same medium supplemented with cefoxitin. No significant differences were observed between the two conditions. The results are summarized in **Figure 3.12** and **Figure 3.13**. The classification is based on the ratio of optical density of the parent strain to that of the mutant strain. In this fashion, a ratio of 1, which could mean that both strains grew equally or that both failed to grow, was discarded from the figures.

Figure 3.12 shows the compounds to which the RΔCD_*acrA-acrB-tolC* strain is significantly sensitive, i.e. the growth ratio was 1.6 or higher. This criterion required that the parent strain grew close to twice as much as the mutant strain, which was determined by measuring turbidity. Compounds to which the mutant was extremely sensitive, ratio ≥ 2.0, are shown with an asterisk on the left. The results suggest that the RΔCD_*acrA-acrB-tolC* strain is sensitive to acidic pH and certain antimicrobial chemicals, including antibiotics, fungicides, and other unrelated chemicals.

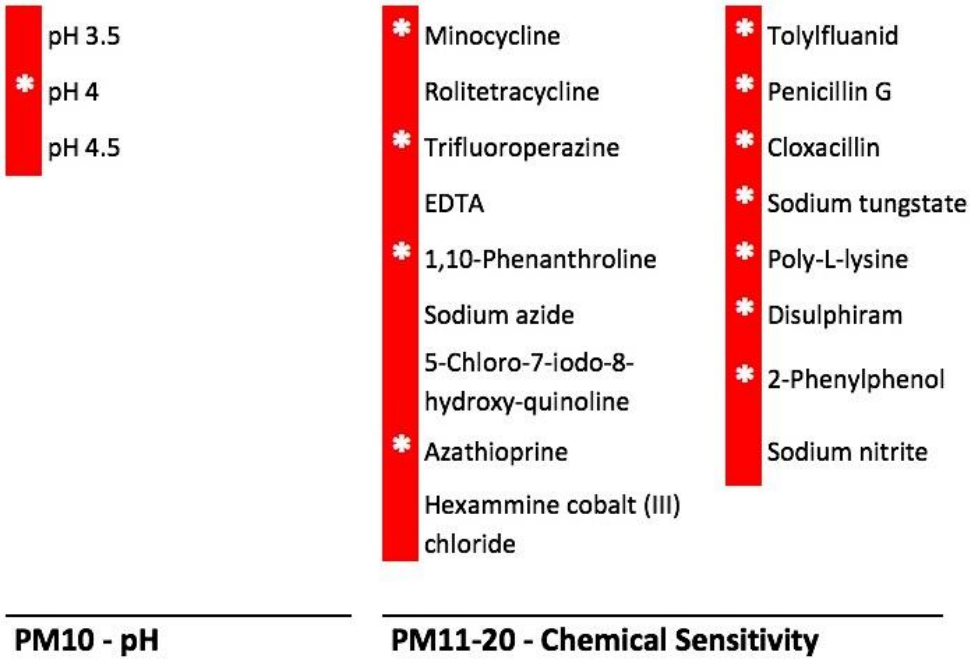

Figure 3.12 - Compounds to which the RΔCD_*acrA-acrB-tolC* strain is sensitive

Summary of the conditions under which there was a significant growth impairment in the R mutant strain. The compounds shown in the figure are further classified in **Chapter 4**.

Figure 3.13 shows the compounds to which the parent R strain is significantly sensitive, i.e. the growth ratio was 0.6 or lower. This criterion required that the mutant strain grew close to twice as much as the parent strain. Compounds to which the parent was extremely sensitive, ratio ≤ 0.4, are shown with an asterisk on the left. The results suggest that the RΔCD_*acrA-acrB-tolC* strain loses sensitivity to certain osmolytes, alkaline pH, and several antimicrobial compounds, including fungicides and antibiotics of the tetracyclines, quinolone, macrolide, and penicillin families.

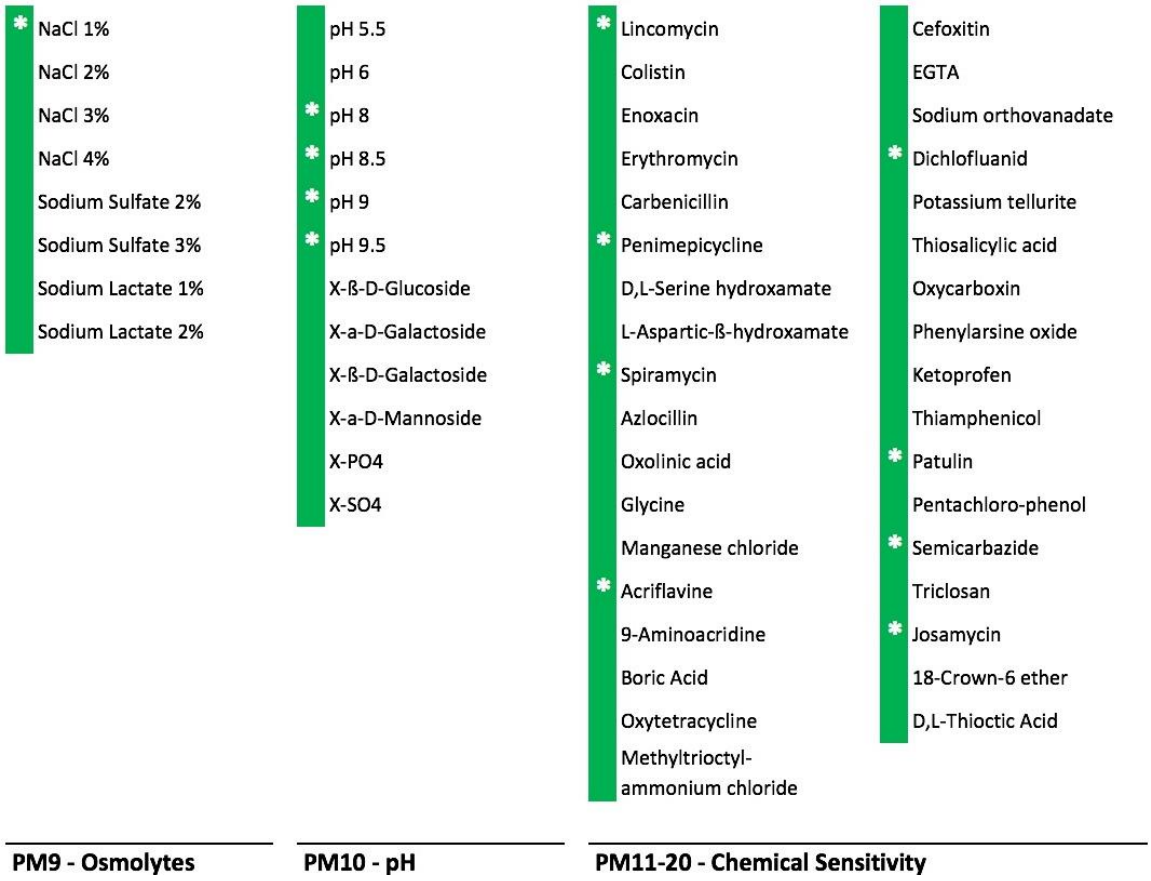

Figure 3.13 - Compounds to which the parent R strain is sensitive

Summary of the conditions under which there was a significant growth impairment in the R parent strain or growth improvement in the R mutant strain. The compounds shown in the figure are further classified in **Chapter 4**.

Alkaline pH Response Assays

A differential response observed with the PM assays was growth patterns under different pH conditions. To study how the mutants respond to different pH conditions, TY medium was prepared adjusting its pH with 5N HCl, to produce a more acidic medium, or 10N NaOH, to produce a more alkaline medium. The growth curves were constructed as previously described. Although the PM assays show that there is a different tolerance to acidic medium between the parent and the RΔCD_*acrA-acrB-tolC* strains, it was not possible to replicate this at pH 4.5 or pH 5. In both cases the bacteria failed to grow. The TY medium probably undergoes chemical

reactions that prevents bacterial growth, and those chemical changes might not be present in the proprietary medium used in the PM assays. The cells, however, could grow in alkaline TY medium. **Figure 3.14** shows the growth curves of the J strains in TY medium at pH 10.0. Under this condition, the parent strain's growth is significantly impaired. The J mutants, however, achieve stationary growth levels comparable to that observed in standard TY medium. The cells were observed microscopically to screen for any morphological changes (**Figure 3.15**). The J parent strain looks completely distorted in this environment. The cells appear as rings instead of the usual rod shape. The mutant strains exhibit some of this morphology, however, the majority of cells appear normal.

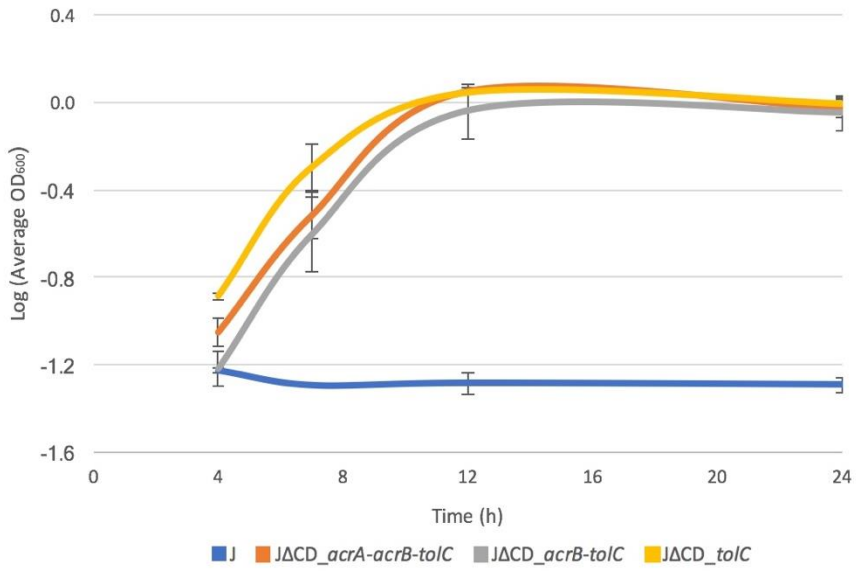

Figure 3.14 - J strains grown in TY medium at pH 10.0

Growth curves of *C. difficile* J strains grown anaerobically in TY medium with pH adjusted to 10.0. The values shown correspond to the log of the average OD_{600} at different time points.

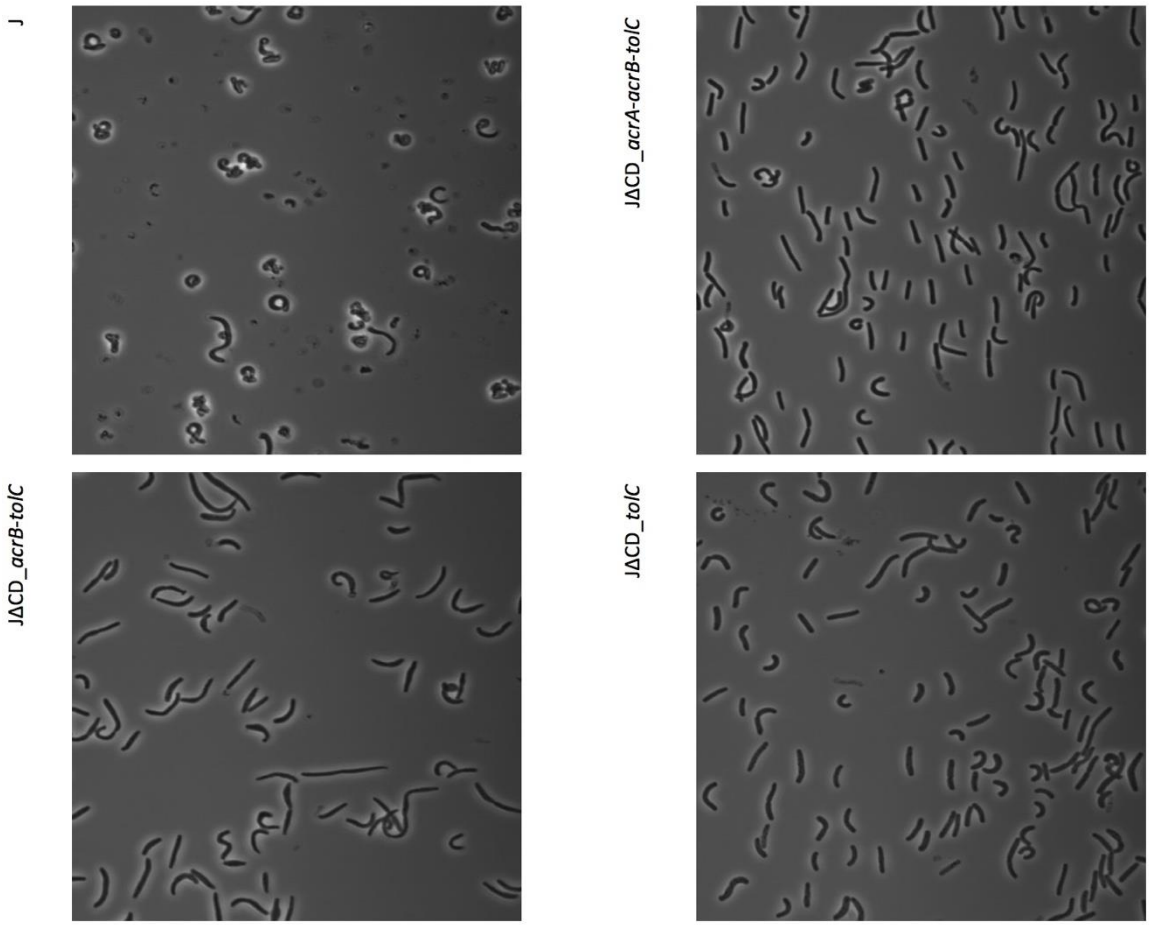

Figure 3.15 – Images of the J strains grown in alkaline TY medium

Phase-contrast images of the J strains after 24 hours of growth in TY broth with pH adjusted to 10.0.

Figure 3.16 shows the growth curves of the R strains in TY medium at pH 10.0. The R parent strain's growth is also impaired in the alkaline medium, although not to the same extent as with the J parent strain. The RΔCD_*acrA-acrB-tolC* and RΔCD_*tolC* strains grow as successfully as the J mutants in the alkaline medium. The cells were also observed microscopically to screen for any morphological changes. The R strain, although achieves a low level of growth, looks completely distorted in this environment. The cells appear as rings instead of the usual rod shape. The mutant strains exhibit some of this morphology, however, the majority of cells appear normal.

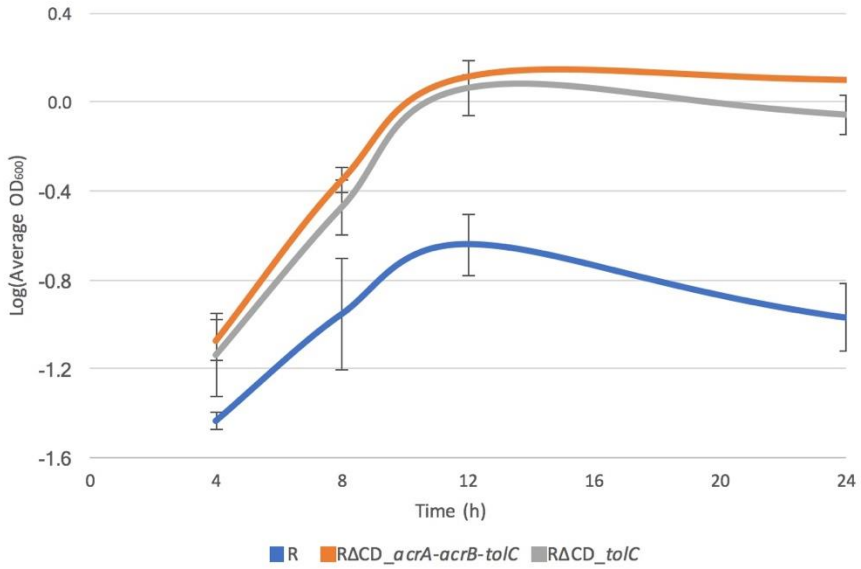

Figure 3.16 - R strains grown in TY medium at pH 10.0

Growth curves of *C. difficile* R strains grown anaerobically in TY medium with pH adjusted to 10.0. The values shown correspond to the log of the average OD_{600} at different time points.

NaCl Response Assays

The PM assays also showed that different NaCl concentrations affected the R and RΔCD_*acrA-acrB-tolC* differently and it was assumed that the same phenotype would occur in the J strains. Growth curves were constructed using TY medium supplemented with different concentrations of NaCl. The following figures correspond to the conditions in which there was a significant growth difference, or, if there was no difference, the maximum NaCl concentration in which the cells could grow. **Figure 3.17** shows the growth patterns of the different J (**A**) and R (**B**) strains grown in TY medium supplemented with 0.2 M NaCl. No significant differences were observed in the J strains, except for a slightly faster reduction of growth at later stationary phase in the mutant strains. This observation closely matched the growth patterns in standard TY medium. Note that it was experimentally determined that this NaCl concentration is the maximum concentration that allows growth of any J strain. For the R strains at this concentration

of NaCl the growth at the exponential phase of the mutants seems to be reduced. However, once the cells reached exponential phase, the growth patterns are identical.

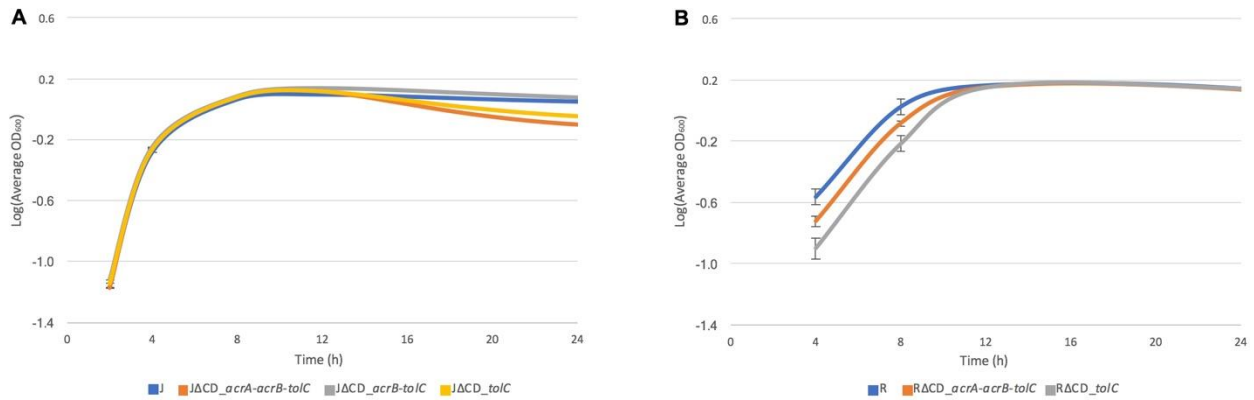

Figure 3.17 - J and R strains grown in TY medium supplemented with 0.2 M NaCl

Growth curves of *C. difficile* strains (A) J and (B) R grown anaerobically in TY medium supplemented with 0.2 M NaCl. The values shown correspond to the log of the average OD_{600} at different time points.

The same experiment was carried out for the R strains at the higher concentration of NaCl (0.45M). Under this condition (**Figure 3.18**), there is a striking difference in growth compared to the lower concentration or standard TY medium. The RΔCD_*tolC* seem to survive well in the high NaCl medium, although growth is significantly slowed down. The ΔCD_*acrA-acrB-tolC strain* had an intermediate survival. In addition to this, it was observed microscopically that the parent strain had severe morphological distortions (not shown). These distortions were not observed in the ΔCD_*tolC* strain. The ΔCD_*acrA-acrB-tolC strain* had an intermediate phenotype.

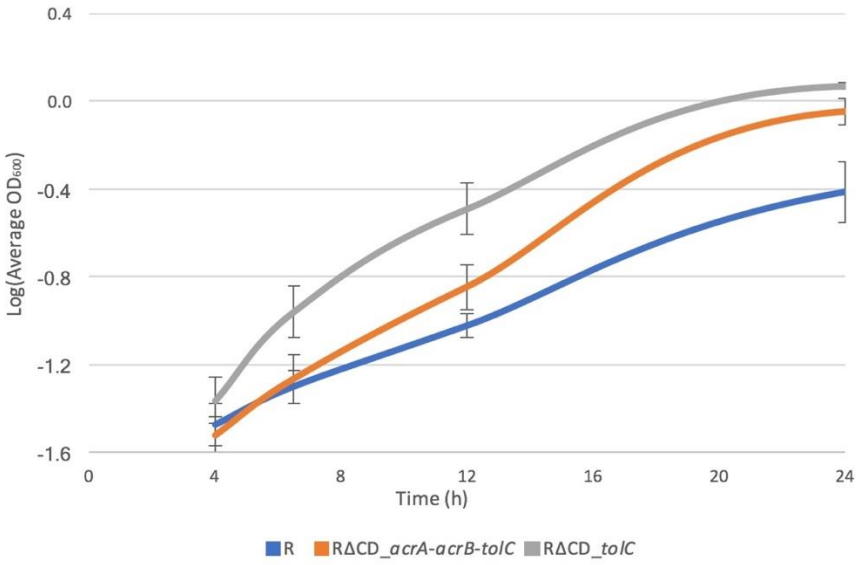

Figure 3.18 - R strains grown in TY medium supplemented with 0.45 M NaCl

Growth curves of *C. difficile* R strains grown anaerobically in TY medium supplemented with 0.45 M NaCl. The values shown correspond to the log of the average OD_{600} at different time points.

Since NaCl causes differential growth phenotypes in the R strains, it was hypothesized that high concentrations NaCl, which represents an adverse environment for the cells, would cause an increase in sporulation in those strains that showed slower growth in this medium, namely the parent strain and the RΔCD_*acrA-acrB-tolC* strain. **Figure 3.19** shows the spore counts in the different R strains grown in TY medium supplemented with different NaCl concentrations. The same sporulation pattern showed previously (RΔCD_*acrA-acrB-tolC* with the most spores, RΔCD_*tolC* with an intermediate number, and R with the least spores) was observed. Surprisingly, with increasing NaCl concentrations a smaller number of spores were observed in all strains, although the relative sporulation levels hold true. The quantification shown in **Figure 3.19** corresponds to the spore counts after 4 days of growth. No significant differences were observed between the spore count after fewer or more days. This experiment was not done for the J strains.

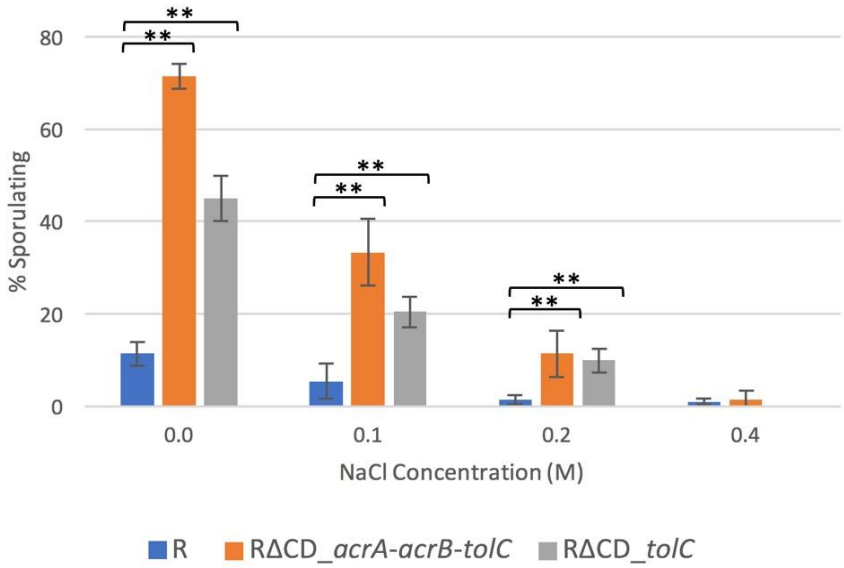

Figure 3.19 - Sporulation efficiency of the R strains in high salinity medium

Spore counts of the R strains grown anaerobically for 4 days in TY plates supplemented with different NaCl concentrations. The values shown correspond to the average spore:vegetative cell ratio of five fields.

Sodium affects the growth of the different strains. It was hypothesized that the growth differences could be related to different intracellular sodium concentrations caused by either the inability of the mutant strains to extrude excess sodium or by their inability to import necessary sodium. In order to study these possibilities, ICP-OES analyses (see **Chapter 2**) were carried out in the different J and R strains grown in either TY medium or TY medium supplemented with NaCl. **Figure 3.20** shows the intracellular concentrations (in ppm) of sodium ions in the different J strains grown in TY medium (**A**) and TY medium supplemented with 0.2 M NaCl (**B**). There seems to be some variation in the intracellular concentration of sodium in standard TY medium. When the J strains are exposed to higher NaCl concentration in the medium, the JΔCD_*acrA-acrB-tolC* strain has a reduced intracellular concentration of sodium compared to the other

strains in the same conditions. However, as shown before, there is essentially no growth difference under this condition.

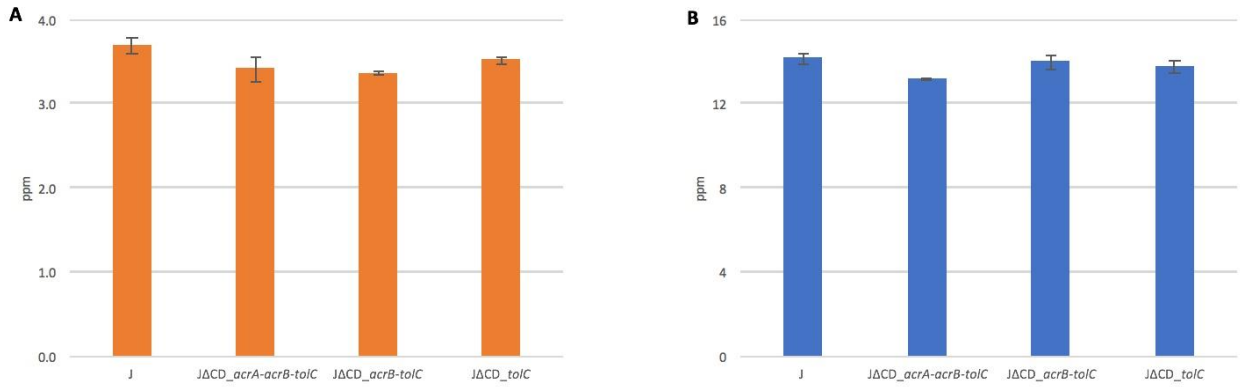

Figure 3.20 - Intracellular Na^+ concentration in the J strains

ICP-OES analysis of intracellular sodium ion concentrations in the J strains grown anaerobically in (A) TY medium and (B) TY medium supplemented with 0.2 M NaCl.

Similarly, **Figure 3.21** shows the intracellular concentrations (in ppm) of sodium ions in the different R strains grown in TY medium (**A**) and TY medium supplemented with 0.45 M NaCl (**B**). There here is more variation of intracellular sodium in TY medium compared to the J strains. The RΔCD_*tolC* strain had a higher concentration of sodium. Note that the concentrations of sodium were significantly lower compared to the J strains. Interestingly, when the R strains are exposed to the high concentration NaCl medium, condition in which there is a growth difference, the intracellular sodium concentrations between the strains vary drastically. The parent R had the highest intracellular concentration, which could be related to its poor survival in high NaCl medium. And the RΔCD_*acrA-acrB-tolC* and RΔCD_*tolC* strains, which had the greatest growth in NaCl medium, had the lowest intracellular sodium concentration.

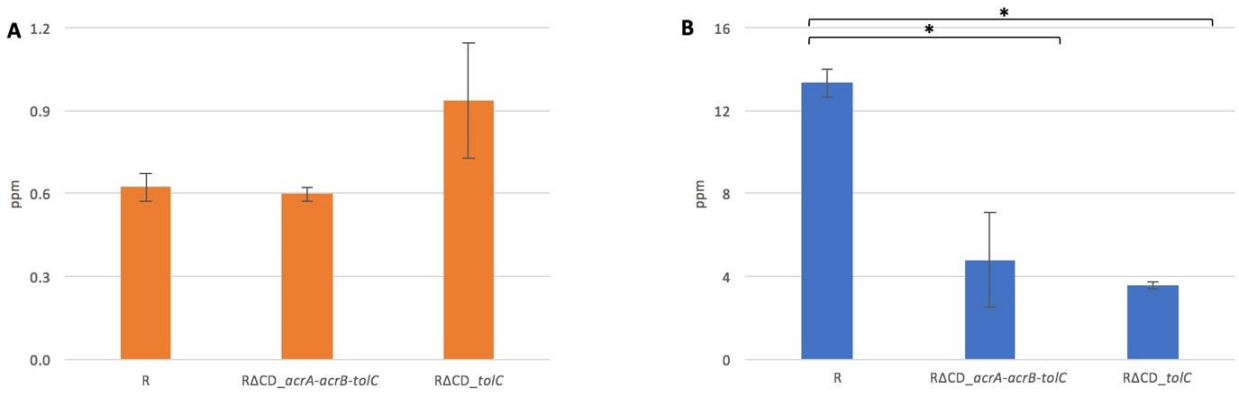

Figure 3.21 - Intracellular Na^+ concentration in the R strains

ICP-OES analysis of intracellular sodium ion concentrations in the R strains grown anaerobically in (A) TY medium and (B) TY medium supplemented with 0.45 M NaCl.

Chapter 4 - Discussion

Structure

Although BLAST analysis shows that CD_AcrA, CD_AcrB, and CD_TolC only have weak homology to their *E. coli* counterparts, I-TASSER structure prediction analysis (**Figure 3.2**) reveals a striking structural similarity between the proteins of these bacteria. It is imperative to obtain crystal structures and confirm or deny the structural inferences made in this project. Due to the striking structure similarities, the mechanistic features observed in previous reports of AcrAB-TolC in *E. coli*, *P. aeruginosa*, and other gram-negative bacteria expressing this complex could be extrapolated to *C. difficile*'s pump complex and thus provide starting points for future studies. For example, in *E. coli*, AcrB substrate binding is mediated by the interaction of the substrate with aromatic residues in the binding pocket, particularly with phenylalanine residues [18]. The binding pocket is readily visible in the predicted structure of CD_AcrB, however, this potential binding pocket is characterized by the absence of phenylalanine residues. Instead, that domain of the predicted structure is rich in tyrosine residues, which could provide aromatic interactions in a similar fashion as the phenylalanine residues in *E. coli*'s AcrB. This could be indications of which residues are important for substrate binding in CD_AcrB and a potential study target for future experiments.

Localization of CD_TolC in *C. difficile*

A high degree of structural similarity suggests that the *C. difficile* proteins are organized in a similar fashion as the gram-negative counterparts. This is conflictive, however, as *C. difficile* lacks an outer-membrane where CD_TolC could localize. Instead, if the organization is the same, CD_TolC should localize in the cell wall. Supporting this idea, Western blot analysis of

extracted surface-layer and cell wall proteins (**Figure 3.6**) reveals that CD_ TolC can be extracted by the same method as surface-layer proteins and cell wall proteins, suggesting that CD_TolC is a cell wall associated protein. However, Western blot analysis of membrane preparations (**Figure 3.5**) indicate that CD_TolC can be extracted with membrane proteins. This observation does not support the idea that these three proteins are organized tandemly as in *E. coli*, instead, CD_TolC would be parallel with CD_AcrB in the membrane. It is plausible that CD_TolC is weakly associated with the peptidoglycan layer and that the detergent used to separate membrane proteins (CD_AcrA and CD_AcrB) from cell wall proteins (CD_TolC) can easily disrupt that association, thus making it appear as if CD_TolC was a membrane protein. Alternatively, if CD_TolC can be expressed as a cell wall protein and a membrane protein, therefore leaving an incomplete complex with only CD_AcrA and CD_AcrB under certain conditions, then the new complex could perform different functions. Interestingly, there have been reports of *E. coli* AcrB performing functions in the regulation of cell growth without interacting with TolC or AcrA [46].

Phenotyping

One initial question asked in this project was whether these genes were essential for the survival and growth of *C. difficile*. **Figure 3.7** shows that the mutant strains can grow in TY medium to levels comparable to that of the parent strains. The increase in sporulation phenotype observed in **Figure 3.9** indicates that the mutants are sensing an adverse growth environment. This could indicate that factors responsible for the regulation of sporulation are affected in the mutant, or that the mutants accumulate toxic materials that lead to the upregulation of sporulation. In **Figure 3.10** it was observed that supplementing the growth medium with

cefoxitin and thus inhibiting sporulation lead to morphological abnormalities. It was hypothesized that these abnormalities could be caused by the accumulation of materials. However, no growth impairment was observed under that condition (**Figure 3.8**). The growth patterns at late stationary phase could give clues about the functions of this protein complex. Under those conditions, there is a reduced nutrient availability in the medium compared to the initial conditions. A faster reduction in growth observed at 12 hours and later in the mutants, particularly the ΔCD_*tolC*, could indicate that CD_AcrA, CD_AcrB, or CD_TolC are involved directly or indirectly in pathways participating in the adaptation to the more limited nutrient availability during stationary phase.

PM Assays

Due to the large number of functions that AcrAB-TolC can perform and the variety of known substrates that have been previously reported, phenotypic microarray assays (Biolog) were performed to attempt to identify the substrates of CD_AcrA-AcrB-TolC. It was hypothesized that if an antimicrobial is a CD_AcrA-AcrB-TolC substrate then the triple mutant would fail to grow under that condition. As seen in **Figure 3.12,** the triple mutant became sensitive to acidic pH conditions and a small number of antimicrobials, including inorganic compounds, organic compounds, fungicides, and antibiotics.

Most of the inorganic compounds contain sodium, and many do not have relevant medical or biocidal uses, except for sodium azide. However, that compound was shown to not affect many gram-positive bacteria, including several *Clostridium* species [47, 48]. In *E. coli*, the mechanism of action of sodium azide is by inhibition of the SecA subunit of the Sec secretory pathway [49]. A homolog of this secretory pathway can be found in *C. difficile* [50]. This might

indicate that sodium azide could have a common target for SecA and CD_AcrA-AcrB-TolC, and that, in the absence of the pump, the Sec pathway might be severely affected as it is the only target for the antimicrobial.

Antibiotics include tetracyclines (minocycline and rolitetracyline) and penicillins (cloxacillin and penicillin G). Penicillins block bacterial division or kill bacteria by inhibition of the formation of peptidoglycan cross-links in the cell wall [51]. This suggests that the efflux pump could be used to extrude these penicillins or that, in the absence of the pump, the antibiotics could reach their targets more efficiently. Tetracyclines inhibit bacterial protein synthesis by interfering with the association of tRNA with the ribosome [52]. This result suggests that the efflux pump could have a direct role in the extrusion of these tetracyclines.

Fungicides include: 2-phenylphenol and tolylfluanid. Interestingly, it was reported that 2-phenylphenol inactivates spores in *C. difficile* [53] and other *Clostridium species* [54]. And the organic compounds include: trifluoroperazine, disulphiram, EDTA, 5-chloro-7-iodo-8-hydroxyquinoline, phenalthroline, poly-L-lysine, and azathioprine. None of these compounds have been reported to act as antimicrobials or to interfere with physiological pathways in *C. difficile*.

An even larger number of conditions to which the triple mutant is tolerant was found. This was summarized in **Figure 3.13** and include: higher NaCl in the medium, alkaline pH, fungicides, and antibiotics. Regarding the different pH conditions, a number of chemicals were tested to assess the activity of different glycoside hydrolases, including glucosidase, galactosidase, and mannosidase. For these conditions, a higher optical density most likely correlates with higher precipitate densities caused by the enzymatic activities rather than with growth. The results suggest that these enzymes are more active in the mutant, and this, in turn,

indicates that the intracellular pH of the mutant might be different than that of the parent as the activity some of these enzymes have been described to be pH dependent in other organisms [55].

A larger number of antibiotics seem to lose effect or promote growth of the triple mutant. This is intriguing, as the initial hypotheses attributed the CD_AcrA-AcrB-TolC complex a primary role in antibiotic resistance. As expected, the parent strain failed to grow in the different lincomycin conditions. This, and growth of the mutant in the presence of other macrolides, can be attributed to the presence of the erythromycin resistance gene in the intron and not to the lack of the pump complex. Other antibiotics include, penicillins, tetracyclines, macrolides, quinolones, thiamphenicol, colistin, and cefoxitin. Interestingly, carbenicillin and azlocillin, two penicillin antibiotics, do not impair growth of the parent, but promote growth in the triple mutant. Two tetracycline antibiotics were identified, oxytetracycline, which has a similar effect as the penicillins, and penimepicycline, which does impair growth in the parent. Two quinolones were identified, enoxacin and oxolinic acid, both of which greatly promote the growth of the mutant. In addition to these antibiotics, colistin, thiamphenicol, and cefoxitin were also identified as promoting growth in the mutant.

Several other compounds affecting the strains differentially were identified too including: antiseptics (acriflavine), dyes (9-aminoacridine), chelating agents (EGTA), fungicides (dichlofluanid, oxycarboxin, pentachlorophenol, triclosan), organic compounds, and inorganic compounds.

Alkaline pH Response

Alkaline conditions were further tested as they could reveal important information about the mechanisms of CD_AcrA-AcrB-TolC, as *E.* coli's AcrB depends on the proton-motive force

to transport substrates to TolC and outside of the cell [56]. **Figure 3.14** and **Figure 3.16** show the growth curves for the J and R strains, respectively, in TY broth with the pH adjusted to 10.0 at the time it was made. Note that it was discovered that the broth undergoes a quick drop in pH once it is put inside the anaerobic chamber. It was determined that after 2 days the pH of the medium dropped to 8.4, and that after this drop the pH remained stable. Nevertheless, the figures and discussion throughout this project refer to those results as obtained in TY medium at pH 10.0, as it was originally adjusted to that pH. The results indicate that the mutants lose sensitivity to alkaline conditions. Indeed, **Figure 3.15** shows that the mutant strains conserved the normal bacterial morphology (compared to **Figure 3.9**, for example) to a great extent. This could indicate that the mutants lack structural features that are prone for denaturation in alkaline conditions, suggesting that the efflux pump participates in the transport of these structural features or, more directly, that the pump itself is denatured in the parent strain. This data also suggests that the mutants are able to adapt to this condition more efficiently, as there are multiple mechanisms for bacterial adaptation to alkaline pH conditions, including upregulation of enzymes that promote proton retention, metabolic changes leading to increased acid production to neutralize alkalinity, and changes in the cell surface layer that promote proton retention [57]. A functional CD_AcrA-AcrB-TolC pump could be responsible for loss of protons in the parent strains, and a mutant lacking this pump would survive better in alkaline conditions.

NaCl Response

High salinity conditions were further studied because of its possible relationship with the morphology changes observed initially in **Figure 3.10**. It was hypothesized that the morphology could be caused by the inability of the mutants to perform osmoregulation and that the bulges

observed were accumulation of materials. If that is the case, the resistance to high NaCl conditions of the mutants, particularly those in the R background, can be attributed to those accumulations, which might act as osmoprotectants. Initially, different NaCl concentrations were tested to assess the ability of the strains to grow. It was determined that the J strains can grow in TY medium supplemented with up to a final concentration of 0.2 M NaCl and that the R strains can grow in medium supplemented with up to a final concentration of 0.45 M NaCl (data not shown). Then, growth curves were constructed for the J and R strains in TY supplemented with 0.2 M NaCl (**Figure 3.17)** and for the R stains in TY supplemented with 0.45 M NaCl (**Figure 3.18)**. **Figure 3.17** shows that the growth patterns for both the J and R strains are similar to that obtained in standard TY medium, including the faster reduction in growth during stationary phase observed in the J mutants before. This could indicate again a poor adaptation to nutrient availability at that growth stage. **Figure 3.18** shows that there is a differential growth pattern in the R strains at a higher NaCl concentrations, condition in which the mutant strains grow more successfully than the parent strain. Note too that the exponential phase is greatly slowed down and that all strains never achieve stationary growth levels comparable to growth in standard TY medium. This could be caused by high intracellular sodium concentrations, as they can impair normal cell functions [58]. And the slowed down growth stages could be caused by a slow adaptation to the adverse conditions, i.e. the time it takes the bacterium to activate pathways that can metabolize or extrude sodium.

Since growth was affected in all strains, clearly indicating that NaCl in the medium represented an adverse condition, it was hypothesized that sporulation would be greatly increased. **Figure 3.19** shows the spore quantification of the R strains grown in medium containing different NaCl concentrations. Although the relative sporulation levels were

maintained, i.e. the triple mutant had the highest spore count followed by the CD_*tolC* mutant and the parent strain, the spore counts decreased greatly with increasing NaCl in the medium. This data suggests that NaCl can act as an inhibitor of sporulation. This inhibition or the mechanism thereof has not been reported in *C. difficile*. However, responses to NaCl has been reported in *Bacillus subtilis* [59, 60] and *Clostridium botulinum* [61], where spores had lower heat resistance and slower germination rates in the presence of NaCl, suggesting that spores are structurally weaker under these conditions and that NaCl might block germination receptors.

Although sporulation is severely impaired in high NaCl medium, vegetative cells can grow to a certain extent. It was hypothesized that the ability of the mutants to grow in the high salinity medium could be caused by the inherent accumulation of salts or other compounds which could counteract the changed osmolarity. To explore this idea, ICP-OES was used to attempt to quantify the intracellular sodium concentrations in the different strains. **Figure 3.20** shows the intracellular concentrations of sodium in the different J strains. No statistically significant difference was observed between the strains, whether they were exposed to normal (**A**) or high (**B**) salinity conditions. **Figure 3.21** shows the concentrations for the R strains. No statistically significant differences were observed in standard TY medium (**A**), suggesting that the R strains do not inherently accumulate sodium. Under high salinity conditions (**B**), however, there is a significant difference between the mutants and the parent strain, in which the sodium concentrations are almost three times higher. This could suggest that the mutants are less permeable to sodium, and that the more successful growth observed in **Figure 3.18** is related to its lower intracellular sodium concentration. In *E. coli*, it was reported that NaCl stress results in accumulation of intracellular sodium as a result of a substantial leak of potassium [62].

Intracellular potassium levels were measure by ICP-OES too, but no significant difference was observed in any strain or growth condition (data not shown).

Summary and Concluding Remarks

The presence of a gram-negative efflux pump complex homolog in *C. difficile* is intriguing. The goal of this project was to provide initial insights into the roles and mechanisms of this complex. To do this, a number of experiments were designed to provide information about the structures, localization, and functions of this protein complex. Based on predicted structures, it was determined that CD_AcrA, CD_AcrB, and CD_TolC have striking structural resemblance to *E. coli* AcrA, AcrB, and TolC, respectively. This, in turn, suggests that the functions and mechanisms of the *C. difficile* efflux pump might be similar to that of the *E. coli* pump. It was determined that acidic pH conditions and a small number of antimicrobials, including inorganic compounds, organic compounds, fungicides, and antibiotics, inhibit growth of a *C. difficile* mutant lacking this pump. Interestingly, higher NaCl in the medium and alkaline pH seem to promote the growth of a *C. difficile* mutant lacking this pump or, surprisingly, only inhibit growth of the wild type strain. The experiments performed in this project suggest that the CD_AcrA-AcrB-TolC efflux pump might have an essential role in *C. difficile* physiology, possibly by serving as an efflux pump for toxic metabolites.

Appendix A - Strains, Plasmids, and Oligonucleotides

Table A.1 - Bacterial Strains

Strain	Description	Source
Escherichia coli DH5α	*E. coli* competent cell	NEB
Escherichia coli S17	*E. coli* competent cell for conjugation with *C. difficile*	[63]
Escherichia coli NEB 10-beta	*E. coli* high efficiency competent cell	NEB
Escherichia coli Rosetta (DE3)	BL21 derivative *E. coli* competent cell for protein expression	MilliporeSigma
Clostridium difficile JIR8094	Erythromycin sensitive derivate of *C. difficile* 630 strain	[64]
Clostridium difficile JIR8094 mutant 678	*C. difficile* strain with intron insertion within the CD630_24060 gene	This study
Clostridium difficile JIR8094 mutant 78	*C. difficile* strain with intron insertion within the CD630_24070 gene	This study
Clostridium difficile JIR8094 mutant 78	*C. difficile* strain with intron insertion within the CD630_24080 gene	This study
Clostridium difficile R20291	R027 epidemic strain	[65]
Clostridium difficile R20291 mutant 678	*C. difficile* strain with intron insertion within the CDR20291_2296 gene	This study
Clostridium difficile R20291 mutant 8	*C. difficile* strain with intron insertion within the CDR20291_2298 gene	This study

Table A.2 - Plasmids

Plasmid name	Backbone	Description	Source
pRGL49	pMTL007C-E5	Plasmid carrying CD630_24060 and CDR20291_2296 intron	This study
pRGL362	pMTL007C-E5	Plasmid carrying CD630_24070 specific intron	This study
pRGL363	pMTL007C-E5	Plasmid carrying CDR20291_2297 specific intron	This study
pRGL89	pMTL007C-E5	Plasmid carrying CD630_24080 and CDR20291_2298 intron	This study
pRPF185	pRPF185	E. coli-C. difficile shuttle vector with tetracycline-inducible promoter	[50]

pRGL364	pGEM-T	Plasmid carrying CD_24080 for cloning into pRPF185	This study
pRGL365	pRFP185	Plasmid carrying CD_24080 with tetracycline inducible promoter	This study
pRGL69	pJ401	CD630_24060 with FLAG-Tag	This study
pRGL70	pJ401	CD630_24070 with Strep-Tag	This study
pRGL66	pJ401	CD630_24080 with His-Tag	This study

Table A.3 - Oligonucleotides

Primer name	**Description**	**Sequence**
ORG566	CD630_24060 with SacI and ribosomal binding site (forward)	GAG CTC GGA GGA GAT ATG AAA AGA TAT TTA ATA GTT TTC TTA ATG TGTA
ORG565	CD630_24060 with XhoI (reverse)	CTC GAG CTT CTC CTT TTC TAC AGG AAA TAT CTT AGT TCC GTC
ORG638	CD630_24070 with SacI and ribosomal binding site (forward)	TTA GAG CTC GGA GAA GTA GAC TAT GAA TTT AAC ACA GAC TTC CGT TAA A
ORG639	CD630_24070 with XhoI (reverse)	TTA TCT CGA GAA CTT TAG CTT TCA ATT TTG GTT TCT TTA TTA
ORG570	CD630_24080 with SacI and ribosomal binding site (forward)	GAG CTC GGA GGG TGA TTG TAT TGA ATA AAA AAA TGA GCA AAA TAG TTG CA
ORG683	CD630_24080 with BamHI (reverse)	AAG TTT TAT TAA AAC TTA TAG GAT CCT TAT TTT CCA GTA TTA AGT ATC CAA G
EBS Universal	Intron specific primer	CGA AAT TAG AAA CTT GCG TTC AGT AAA C

Appendix B - Supplemental Data

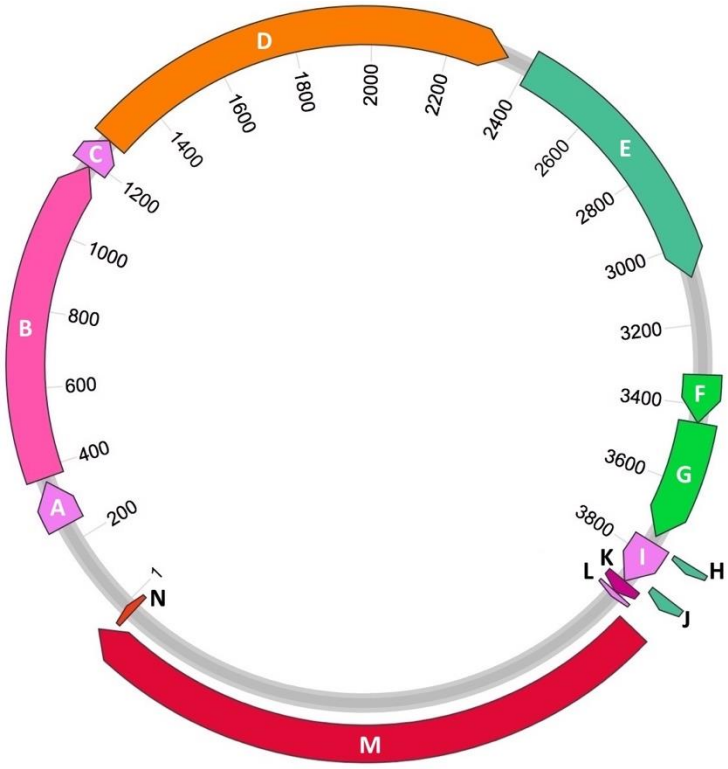

Figure B.1 - Expression plasmids synthesized by ATUM

A: Promoter; B: Kanamycin resistance gene; C: Promoter; D: Transcriptional repressor *lacI;* E: Origin of replication; F: Transcriptional terminator; G: Transcriptional terminator; H: Operator sequence; I: T5 inducible promoter; J: Operator sequence; K: T7 5' UTR; L: Ribosomal binding site; M: Insert; N: Tag. For pRGL69, M is CD630_24060 (1,268 bp) and N is FLAG-tag. For pRGL70, M is CD630_24070 (3,249 bp) and N is Strep-tag. For pRGL66, M is CD_630_24080 (1,358 bp) and N is 6XHis-Tag. Adapted from the DNA ATLAS map provided by ATUM (Newark, CA).

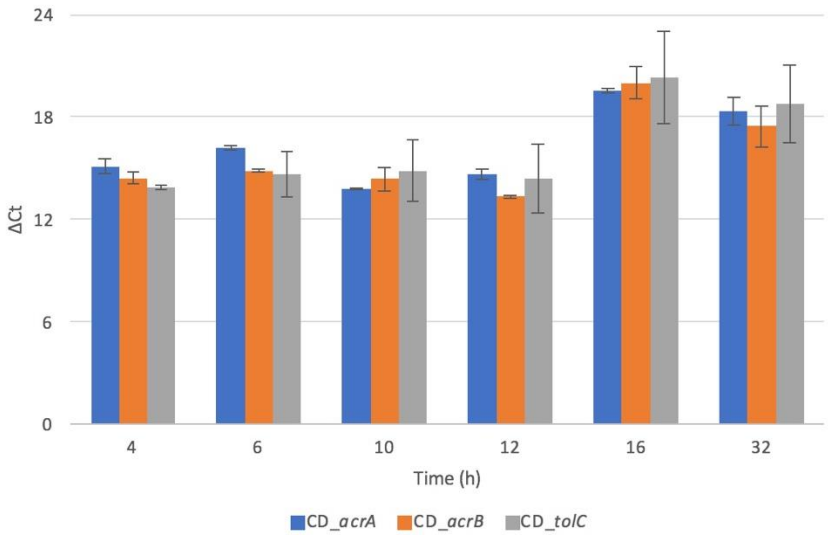

Figure B.2 - RT-PCR

Normalized expression of CD_*acrA*, CD_*acrB*, and CD_*tolC* in the J strain in TY medium. Maximum transcript abundance is shown by the lowest ΔCt value. Experiment performed by Brintha Parasumanna Girinathan (unpublished).

References

1. Dolgin, E., *'Game Changer' Antibiotic and Others in Works for Superbug.* Nature Medicine, 2011. **17**(1): p. 10.

2. Just, I., et al., *Glucosylation of Rho Proteins by Clostridium difficile Toxin B.* Nature, 1995. **375**(6531): p. 500-503.

3. Mukherjee, K., S. Karlsson, and L. Burman, *Proteins Released During High Toxin Production in Clostridium difficile.* Microbiology, 2002. **148**: p. 2245-2253.

4. Spigaglia, P., *Recent Advances in the Understanding of Antibiotic Resistance in Clostridium difficile Infection.* Therapeutic Advances in Infectious Disease, 2016. **3**(1): p. 23-42.

5. Barlett, J.G., et al., *Role of Clostridium difficile in Antibiotic-associated Pseudomembranous Colitis.* Gastroenterology, 1978. **75**(5): p. 778-782.

6. Dridi, L., J. Tankovic, and J.C. Petit, *CdeA of Clostridium difficile, a New Multidrug Efflux Transporter of the MATE Family.* Microbial Drug Resistance, 2004. **10**(3): p. 191-196.

7. Lebel, S., S. Bouttier, and T. Lambert, *The cme Gene of Clostridium difficile Confers Multidrug Resistance in Enterococcus faecalis.* Microbiology Letters, 2004. **238**(1): p. 93-100.

8. Bannam, T.L., et al., *The Clostridium perfringens TetA(P) Efflux Protein Contains a Functional Variant of the Motif A Region Found in Major Facilitator Superfamily Transport Proteins.* Microbiology, 2004. **150**: p. 127-134.

9. Kazimierczak, K.A., et al., *A New Tetracycline Efflux Gene, tet(40), Is Located in Tandem with tet(O/32/O) in a Human Gut Firmicute Bacterium and in Metagenomic Library Clones.* Antimicrobial Agents and Chemotherapy, 2008. **52**(11): p. 40001-4009.

10. Mousa, J. and D. Bruner, *Structural and Mechanistic Diversity of Multidrug Transporters.* Natural Product Reports, 2016. **33**: p. 1255-1267.

11. Sun, J., Z. Deng, and A. Yan, *Bacterial Multidrug Efflux Pumps: Mechanisms, Physiology and Pharmacological Exploitations.* Biochemical and Biophysical Research Communications, 2014. **453**: p. 254-267.

12. Boetzkes, A., et al., *Secretome Analysis of Clostridium difficile Strains.* Archives of Microbiology, 2012. **194**: p. 675-687.

13. Nikaido, H. and H.I. Zgurskaya, *AcrAB and Related Multidrug Efflux Pumps of Escherichia coli.* Journal of Molecular Microbiology and Biotechnology, 2001. **3**(2): p. 215-218.

14. Nishino, K., E. Nikaido, and A. Yamaguchi, *Regulation and Physiological Function of Multidrug Efflux Pumps in Escherichia coli and Salmonella.* Biochimica et Biophysica Acta, 2009. **1794**(5): p. 834-843.

15. Masuda, N., et al., *Substrate Specificities of MexAB-OprM, MexCD-OprJ, and MexXY-OprM Efflux Pumps in Pseudomonas aeruginosa.* Antimicrobial Agents and Chemotherapy, 2000. **44**(12): p. 3322-3327.

16. Eswaran, J., et al., *Three's Company: Component Structures Bring a Closer View of Tripartite Drug Efflux Pumps.* Current Opinion in Structural Biology, 2004. **14**(6): p. 741-747.

17. Janganan, T.K., et al., *Evidence for the Assembly of a Bacterial Tripartite Multidrug Pump with a Stoichiometry of 3:6:3.* Journal of Biological Chemistry, 2011. **286**: p. 26900-26912.

18. Murakami, S., et al., *Crystal Structures of a Multidrug Transporter Reveal a Functionally Rotating Mechanism.* Nature, 2006. **443**: p. 173-179.

19. Takatsuka, Y. and H. Nikaido, *Covalently Linked Trimer of the AcrB Multidrug Efflux Pump Provides Support for the Functional Rotating Mechanism.* Journal of Bacteriology, 2009. **191**(6): p. 1729-1737.

20. Wang, Z., et al., *An Allosteric Transport Mechanism for the AcrAB-TolC Multidrug Efflux Pump.* Biophysics and Structural Biology, 2017.

21. Thanassi, D., L. Cheng, and N. Nikaido, *Active Efflux of Bile Salts by Escherichia coli.* Journal of Bacteriology, 1997. **179**(8): p. 2512-2518.

22. Piddock, L., et al., *Evidence for an Efflux Pump Mediating Multiple Antibiotic Resistance in Salmonella enterica Serovar Typhimurium.* Antimicrobial Agents and Chemotherapy, 2000. **44**(11): p. 3118-3121.

23. Shafer, W., et al., *Modulation of Neisseria gonorrhoeae Susceptibility to Vertebrate Antibacterial Peptides Due to a Member of the Resistance/Nodulation/Division Efflux Pump Family.* PNAS, 1997. **95**(4): p. 1829-1833.

24. Poole, K., et al., *Overexpression of the mexC–mexD–oprJ Efflux Operon in nfxB-type Multidrug-resistant Strains of Pseudomonas aeruginosa.* Molecular Microbiology, 1996. **21**(4): p. 713-724.

25. Hirakata, Y., et al., *Multidrug Efflux Systems Play an Important Role in the Invasiveness of Pseudomonas aeruginosa.* The Journal of Experimental Medicine, 2002. **196**(1): p. 109.

26. Evans, K., et al., *Influence of the MexAB-OprM Multidrug Efflux System on Quorum Sensing in Pseudomonas aeruginosa.* Journal of Bacteriology, 1998. **180**(20): p. 5443-5447.

27. Köhler, T., et al., *Overexpression of the MexEF-OprN Multidrug Efflux System Affects Cell-to-Cell Signaling in Pseudomonas aeruginosa.* Journal of Bacteriology, 2001. **183**(18): p. 5213-5222.

28. Rahmati, S., et al., *Control of the AcrAB Multidrug Efflux Pump by Quorum-sensing Regulator SdiA.* Molecular Microbiology, 2002. **43**(3): p. 677-685.

29. Kvist, M., V. Hancock, and P. Klemm, *Inactivation of Efflux Pumps Abolishes Bacterial Biofilm Formation.* Applied and Evironmental Microbiology, 2008. **74**(23): p. 7376-7382.

30. Matsumara, K., et al., *Roles of Multidrug Efflux Pumps on the Biofilm Formation of Escherichia coli K-12.* Biocontrol Science, 2011. **16**(2): p. 69-72.

31. Baugh, S., et al., *Loss of or Inhibition of all Multidrug Resistance Efflux Pumps of Salmonella enterica Serovar Typhimurium Results in Impaired Ability to Form a Biofilm.* Journal of Antimicrobial Chemotherapy, 2012. **67**(10): p. 2409-2417.

32. Girinathan, B.P., et al., *Importance of Glutamate Dehydrogenase (GDH) in Clostridium difficile Colonization in Vivo.* PLOS One, 2016. **11**(10).

33. Sirigireddy, A.R., et al., *Identification and Characterization of Clostridium sordellii Toxin Gene Regulator.* Journal of Bacteriology, 2013. **195**(18): p. 4246-4254.

34. Govind, R., L. Fitzwater, and R. Nichols, *Observations on the Role of TcdE Isoforms in Clostridium difficile Toxin Secretion.* Journal of Bacteriology, 2015. **197**(15): p. 2600-2609.

35. Govind, R., et al., *Evidence that Clostridium difficile TcdC Is a Membrane-Associated Protein.* Journal of Bacteriology, 2006. **188**(10): p. 3716-3720.

36. Boel, G., et al., *Codon Influence on Protein Expression in E. coli Correlates with mRNA Levels.* Nature, 2016. **529**(7586): p. 358-363.

37. Heap, J.T., et al., *The ClosTron: A Universal Gene Knock-out System for the Genus Clostridium.* Journal of Microbiological Methods, 2007. **70**(3): p. 452-464.

38. Perutka, J., et al., *Use of Computer-designed Group II Introns to Disrupt Escherichia coli DExH/D-box Protein and DNA Helicase Genes.* Journal of Molecular Biology, 2004. **336**(2): p. 421-439.

39. Govind, R. and B. Dupuy, *Secretion of Clostridium difficile Toxins A and B Requires the Holin-like Protein TcdE.* PLoS Pathogens, 2012. **8**(6).

40. Merrigan, M.M., et al., *Surface-Layer Protein A (SlpA) Is a Major Contributor to Host-Cell Adherence of Clostridium difficile.* PLOS One, 2013. **8**(11): p. e78404.

41. Calabi, E., et al., *Molecular Characterization of the Surface Layer Proteins from Clostridium difficile.* Molecular Microbiology, 2001. **40**(5): p. 1187-1199.

42. Girinathan, B.P., et al., *Effect of tcdR Mutation on Sporulation in the Epidemic Clostridium difficile Strain R20291*. mSphere, 2017. **2**(1): p. e00383-16.

43. Putman, E.E., et al., *SpoIVA and SipL are Clostridium difficile Spore Morphogenetic Proteins.* Journal of Bacteriology, 2013. **195**(6): p. 1214-1225.

44. Burns, D.A. and N.P. Minton, *Sporulation Studies in Clostridium difficile.* Journal of Microbiological Methods, 2011. **87**(2): p. 133-138.

45. Lei, X. and B.R. Bochner, *Using Phenotype MicroArrays to Determine Culture Conditions That Induce or Repress Toxin Production by Clostridium difficile and Other Microorganisms.* PLOS One, 2013. **8**(2): p. e56545.

46. Aoki, S.K., et al., *Contact-dependent Growth Inhibition Requires the Essential Outer Membrane Protein BamA (YaeT) as the Receptor and the Inner Membrane Transport Protein AcrB.* Molecular Microbiology, 2008. **70**(2): p. 323-340.

47. Lichstein, H.C. and M.H. Soule, *Studies of the Effect of Sodium Azide on Microbic Growth and Respiration.* Journal of Bacteriology, 1944. **47**(3): p. 239-251.

48. Gerencser, V.F. and R.H. Weaver, *A New Technique for the Use of Sodium Azide (Hydrazoic Acid) as an Inhibitive Agent.* Applied Microbiology, 1959. **7**(2): p. 113-115.

49. Fortin, Y., P. Phoenix, and G.R. Drapeau, *Mutations Conferring Resistance to Azide in Escherichia coli Occur Primarily in the secA Gene.* Journal of Bacteriology, 1990. **172**(11): p. 6607-6610.

50. Fagan, R.P. and N.F. Fairweather, *Clostridium difficile Has Two Parallel and Essential Sec Secretion Systems.* Journal of Biological Chemistry, 2011. **286**(31): p. 27493-27493.

51. Yocum, R.R., J.R. Rasmussen, and J.L. Strominger, *The Mechanism of Action of Penicillin. Penicillin Acylates the Active Site of Bacillus stearothermophilus D-alanine Carboxypeptidase.* Journal of Biological Chemistry, 1980. **255**(9): p. 3977.

52. Chopra, I. and M. Roberts, *Tetracycline Antibiotics: Mode of Action, Applications, Molecular Biology, and Epidemiology of Bacterial Resistance.* Microbiology and Molecular Biology Reviews, 2001. **65**(2): p. 232-260.

53. Tutala, W.A., M.F. Gergen, and D.J. Weber, *Inactivation of Clostridium difficile Spores by Disinfectants.* Infection Control & Hospital Epidemiology, 1993. **14**(1): p. 36-39.

54. Cha, C., Y. Cho, and H. Lee, *Sporicidal Efficacy of a Fumigation Disinfectant Composited to Ortho-phenylphenol Against Spores of Clostridium Perfringens.* Journal of Food Hygiene and Safety, 2014: p. 217-222.

55. Heikinheimo, P., et al., *The Structure of Bovine Lysosomal α-Mannosidase Suggests a Novel Mechanism for Low-pH Activation.* Journal of Molecular Biology, 2003. **327**(3): p. 631-644.

56. Tikhonova, E.B. and H.I. Zgurskaya, *AcrA, AcrB, and TolC of Escherichia coli Form a Stable Intermembrane Multidrug Efflux Complex.* Journal of Biological Chemistry, 2004. **279**(31): p. 32116-32124.

57. Padan, E., et al., *Alkaline pH Homeostasis in Bacteria: New Insights.* Biochimica et Biophysica Acta, 2005. **1717**(2): p. 67-88.

58. Hase, C.C., et al., *Sodium Ion Cycle in Bacterial Pathogens: Evidence from Cross-Genome Comparisons.* Microbiology and Molecular Biology Reviews, 2001. **65**(3): p. 353-370.

59. Fleming, H.P. and Z.J. Ordal, *Responses of Bacillus subtilis Spores to Ionic Environments During Sporulation and Germination.* Journal of Bacteriology, 1964. **88**(6): p. 1529-1537.

60. Nagler, K., et al., *High Salinity Alters the Germination Behavior of Bacillus subtilis Spores with Nutrient and Nonnutrient Germinants.* Applied and Evironmental Microbiology, 2014. **80**(4): p. 1314-1321.

61. Webb, M.D., et al., *Historical and Contemporary NaCl Concentrations Affect the Duration and Distribution of Lag Times from Individual Spores of Nonproteolytic Clostridium botulinum.* Applied and Evironmental Microbiology, 2007. **73**(7): p. 2118-2127.

62. Shabala, L., et al., *Ion Transport and Osmotic Adjustment in Escherichia coli in Response to Ionic and Non-ionic Osmotica.* Environmental Microbiology, 2009. **11**(1): p. 137-148.

63. Teng, F., B.E. Murray, and G.M. Weinstock, *Conjugal Transfer of Plasmid DNA from Escherichia coli to Enterococci: a Method to Make Insertion Mutations.* Plasmid, 1998. **39**(3): p. 182-186.

64. O'Connor, J.R., et al., *Construction and Analysis of Chromosomal Clostridium difficile Mutants.* Molecular Microbiology, 2006. **61**(5): p. 1335-1351.

65. Stabler, R.A., et al., *Comparative Genome and Phenotypic Analysis of Clostridium difficile 027 Strains Provides Insight into the Evolution of a Hypervirulent Bacterium.* Genome Biology, 2009. **10**(9).